

SANDIA REPORT

SAND2003-1964
Unlimited Release
Printed June 2003

Exploring the Feasibility of Fabricating Micron-scale Components using Microcontact Printing

Ramona L. Myers, M. Barry Ritchey, Robert N. Stokes, Adrian L. Casias,
David P. Adams, Andrew D. Oliver, and John A. Emerson

Prepared by
Sandia National Laboratories
Albuquerque, New Mexico 87185 and Livermore, California 94550

Sandia is a multiprogram laboratory operated by Sandia Corporation,
a Lockheed Martin Company, for the United States Department of Energy's
National Nuclear Security Administration under Contract DE-AC04-94AL85000.

Approved for public release; further dissemination unlimited.



Issued by Sandia National Laboratories, operated for the United States Department of Energy by Sandia Corporation.

NOTICE: This report was prepared as an account of work sponsored by an agency of the United States Government. Neither the United States Government, nor any agency thereof, nor any of their employees, nor any of their contractors, subcontractors, or their employees, make any warranty, express or implied, or assume any legal liability or responsibility for the accuracy, completeness, or usefulness of any information, apparatus, product, or process disclosed, or represent that its use would not infringe privately owned rights. Reference herein to any specific commercial product, process, or service by trade name, trademark, manufacturer, or otherwise, does not necessarily constitute or imply its endorsement, recommendation, or favoring by the United States Government, any agency thereof, or any of their contractors or subcontractors. The views and opinions expressed herein do not necessarily state or reflect those of the United States Government, any agency thereof, or any of their contractors.

Printed in the United States of America. This report has been reproduced directly from the best available copy.

Available to DOE and DOE contractors from

U.S. Department of Energy
Office of Scientific and Technical Information
P.O. Box 62
Oak Ridge, TN 37831

Telephone: (865)576-8401
Facsimile: (865)576-5728
E-Mail: reports@adonis.osti.gov
Online ordering: <http://www.doe.gov/bridge>

Available to the public from

U.S. Department of Commerce
National Technical Information Service
5285 Port Royal Rd
Springfield, VA 22161

Telephone: (800)553-6847
Facsimile: (703)605-6900
E-Mail: orders@ntis.fedworld.gov
Online order: <http://www.ntis.gov/help/ordermethods.asp?loc=7-4-0#online>



SAND2003-1964
Unlimited Release
Printed June 2003

Exploring the Feasibility of Fabricating Micron-scale Components using Microcontact Printing

LDRD Final Report

Ramona L. Myers
Nuclear Safety Assessment Department

M. Barry Ritchey
Neutron Tube Design Department

Robert N. Stokes, Adrian L. Casias and David P. Adams
Thin Film, Vacuum, and Packaging Department

Andrew D. Oliver
BEOL Advanced Packaging Department

John A. Emerson
Organic Materials Department

Sandia National Laboratories
P. O. Box 5800
Albuquerque, NM 87185-0492

Abstract

Many microfabrication techniques are being developed for applications in microelectronics, microsensors, and micro-optics. Since the advent of microcomponents, designers have been forced to modify their designs to include limitations of current technology, such as the inability to make three-dimensional structures and the need for piece-part assembly. Many groups have successfully transferred a wide variety of patterns to both two-dimensional and three-dimensional substrates using microcontact printing. Microcontact printing is a technique in which a self-assembled monolayer (SAM) is patterned onto a substrate by transfer printing. The patterned layer can act as an etch resist or a foundation upon which to build new types of microstructures. We created a gold pattern with features as small as 1.2 μm using microcontact printing and subsequent processing. This approach looks promising for constructing single-level structures such as microelectrode arrays and sensors. It can be a viable technique for creating three-dimensional structures such as microcoils and microsprings if the right equipment is available to achieve proper alignment, and if a means is available to connect the final parts to other components in subsequent assembly operations. Microcontact printing provides a wide variety of new opportunities in the fabrication of microcomponents, and increases the options of designers.

Acknowledgments

We value the efforts of Cathy Sifford of the Processing Engineering Department (formerly of the Thin Film, Vacuum, and Packaging Department), and Beverly Silva of the Thin Film, Vacuum, and Packaging Department for coating numerous samples of silicon wafers, glass slides, and glass capillaries. We are grateful to Dave Staley and Troy Gourley of the Thin Film, Vacuum, and Packaging Department for developing a fixture for the evaporation chamber that produces uniform coatings on glass capillaries. In addition, we appreciate their efforts in modifying the fixture to allow more capillaries to be coated simultaneously, to increase throughput. We value the assistance we received from Justin Baca, student intern of the Organic Materials Department, and Yoosuf Picard, student intern of the Thin Film, Vacuum, and Packaging Department.

We appreciate the efforts of Don Greene of the Mechanical Engineering Department and Guy Prevost of the Organic Materials Department in designing and fabricating a fixture for the micromanipulator that securely holds a capillary in position while allowing it to roll over the stamp surface. We are grateful to Chris Sorenson of the Integrated Surety Mechanisms 1 Department (formerly of the Organic Materials Department) for fabricating a mold to make elastomer boots to hold the ends of a capillary in place in the micromanipulator fixture.

We appreciate Darlene Tafoya and Mel Gonzales of the Electronic Fabrication Department for their work in developing a method to attach wires to the flat microcoils. We are grateful to Graham Yelton of the Photonic Microsystems Technology Department for his consultation on the electroplating operations. We really appreciate the use of the chrome photomask loaned to us by Carolyn Matzke of the Microdevice Technologies Department.

Ramona Myers gratefully acknowledges the Nuclear Safety Assessment Department for providing the greater part of the funding to write this report.

Contents

| | |
|--|----|
| Abstract | 3 |
| Acknowledgments | 4 |
| Nomenclature | 8 |
| Introduction: A Robust, Inexpensive Microfabrication Technique Is Needed for Current Designs | 9 |
| Background: Microcontact Printing Has Been Used in a Wide Variety of Applications for Both 2-D and 3-D Substrates | 11 |
| Scope: Many Factors Affect the Integrity of the Final Part | 14 |
| Experimental: Several Tasks Are Required to Produce a Part with Microcontact Printing | 21 |
| Results: Contact Inking is Better than Wet Inking for Transferring Patterns with Fine Features | 27 |
| Conclusions and Recommendations for Future Work: Try Contact Inking with ECT and a Stiffer Stamp Material | 41 |
| References | 44 |

Figures

| | | |
|---|---|----|
| 1 | Diagram of self-assembled alkanethiolate monolayer | 10 |
| 2 | Procedure for microcontact printing on a flat substrate | 10 |
| 3 | Problems from using incorrect aspect ratios in designing a stamp | 15 |
| 4 | Wet inking of a stamp..... | 17 |
| 5 | Diffusion of HDT molecules due to the wet-inking method | 18 |
| 6 | Contact inking of a stamp..... | 19 |
| 7 | Contact inking produces a cleaner pattern transfer than wet inking | 19 |

| | | |
|----|--|----|
| 8 | Special fixture for thin-film deposition of coatings on glass capillaries | 22 |
| 9 | Procedure for creating SU-8 master using photolithography | 22 |
| 10 | Micromanipulator used for printing capillaries | 26 |
| 11 | Fixture for holding capillary in micromanipulator | 26 |
| 12 | Replication of FIB structure with Sylgard 184..... | 29 |
| 13 | Brass master made with a 25- μ m-diameter micro-end-mill tool fabricated by FIB milling | 30 |
| 14 | Sylgard 184 stamp made from brass master..... | 30 |
| 15 | SEM image of HDT monolayer created by microcontact printing | 31 |
| 16 | Two sets of the half-links pattern in silver on a silicon wafer | 31 |
| 17 | Examples of gold patterns on 2-D substrates..... | 32 |
| 18 | Round and square microcoils, after etching and after electroplating..... | 33 |
| 19 | Optical micrograph of silver half-links design on a glass capillary | 34 |
| 20 | SEM image of gold half-links pattern on a glass capillary | 34 |
| 21 | Drawing of the half-links pattern on two adjoined corners..... | 35 |
| 22 | Modified design of the half-links pattern..... | 36 |
| 23 | Microcontact-printing method for transferring the microcoil design to a metallized glass capillary | 36 |
| 24 | Diagram showing the parameters for rolling a capillary on a stamp to print the microcoil pattern | 37 |
| 25 | Etched microcoil pattern in gold on a capillary | 38 |
| 26 | Examples of microcoil defects..... | 38 |

| | | |
|----|---|----|
| 27 | Uneven thickness of the stamp causes discontinuous contact of the capillary during printing..... | 39 |
| 28 | Etched patterns of stick figures printed on a gold substrate using the contact-inking method..... | 40 |
| 29 | Example of a defect due to the stamp skipping on the substrate during printing..... | 40 |
| 30 | The average line width is 1.2 μm for the lines in the “skirt” area of the stick figures shown in Figures 28 and 29 | 41 |

Table

| | | |
|---|---|----|
| 1 | Candidate Materials for Elastomeric Stamp | 28 |
|---|---|----|

Nomenclature

| | |
|------------------|--|
| 2-D | two-dimensional |
| 3-D | three-dimensional |
| AFM | atomic force microscope |
| CCD | charge-coupled detector |
| ECT | eicosanethiol ($\text{CH}_3(\text{CH}_2)_{19}\text{SH}$) |
| FIB | focused ion beam |
| GBL | gamma-butyrolactone |
| $^1\text{H-NMR}$ | proton nuclear magnetic resonance spectroscopy |
| HDT | 1-hexadecanethiol ($\text{CH}_3(\text{CH}_2)_{15}\text{SH}$) |
| HMDS | hexamethyldisilazane |
| LIGA | Lithographie, Galvanoformung, Abformung (German acronym) |
| NiCr | nickel chromium |
| NiAl | nickel aluminum |
| O.D. | outer diameter |
| PDMS | polydimethylsiloxane |
| PGMEA | propylene glycol monomethyl ether acetate |
| PMMA | polymethylmethacrylate |
| SAM | self-assembled monolayer |
| SEM | scanning electron microscope |
| STM | scanning tunneling microscope |
| UV | ultraviolet |
| Contact time | time that inked stamp is in conformal contact with the substrate |
| Inking time | time that ink solution is in contact with the stamp surface |
| Inking pad | flat, smooth (unpatterned) sheet of PDMS used in contact inking |
| Ink solution | solution of alkanethiol in ethanol that is used to ink the stamp |
| Sylgard 184 | Sylgard 184 PDMS (silicone) encapsulant |
| Stamp | PDMS with a patterned surface used in microcontact printing |
| Å | Angstrom (1×10^{-10} meter) |
| cm | centimeter (1×10^{-2} meter) |
| keV | kiloelectron volts |
| kPa | kilopascals (1×10^3 Newton per square meter) |
| mJ | millijoules (1×10^{-3} Newton-meter) |
| ml | milliliter (1×10^{-3} liter) |
| mm | millimeter (1×10^{-3} meter) |
| mM | millimolar (1×10^{-3} moles solute per liter solution) |
| M | molar (moles solute per liter solution) |
| MPa | megapascals (1×10^6 Newton per square meter) |
| nm | nanometer (1×10^{-9} meter) |
| N/mm^2 | Newton per square millimeter |
| rpm | revolutions per minute |
| Torr | millimeter of mercury at 0°C |
| μm | micron (1×10^{-6} meter) |
| Z | atomic number |

Introduction: A Robust, Inexpensive Microfabrication Technique Is Needed for Current Designs

Many microfabrication techniques are being developed for applications in microelectronics, microsensors, and microoptics. Since the advent of microcomponents, designers have been forced to modify their designs to include limitations of current technology, such as the inability to make 3-D structures and the need for piece-part assembly. Microcomponents produced by photolithography are intrinsically two-dimensional (2-D). Numerous and often time-consuming steps are required for product realization in many applications; this results in very expensive components. While many microcomponents have been constructed using silicon-based micromachining and Lithographie, Galvanoformung, Abformung (LIGA), a method is not currently available to fabricate three-dimensional (3-D) microcomponents reproducibly without piece-part assembly. Despite significant progress in these techniques, many 3-D structures remain difficult to construct. In addition, many technologies such as silicon-based surface micromachining are limited to one material. For inexpensive production of microcomponents, a robust technique is needed to fabricate 3-D structures with high precision and good reproducibility.

A set of techniques called “soft lithography” has been developed by George M. Whitesides at Harvard University (see Xia and Whitesides [1] for a review article). These soft-lithographic techniques all involve the transfer of a pattern to a substrate using an elastomer such as polydimethylsiloxane (PDMS) as a stamp, mask, or mold. In general, these techniques are inexpensive, experimentally convenient, and readily accessible to scientists and engineers; they can often be done in an ambient laboratory environment. Soft-lithographic methods are promising techniques that are being pursued for a manufacturing environment since they do not require special equipment like a synchrotron radiation facility, as required for LIGA. Furthermore, they have the capability to make 3-D microcomponents without piece-part assembly for a wide variety of materials including metals, ceramics, and polymers. Soft-lithographic methods can give designers much more freedom in designing 3-D microcomponents to meet increasingly demanding customer requirements.

Microcontact printing is a soft-lithographic technique in which a self-assembled monolayer (SAM) is patterned onto a substrate by transfer printing. A SAM forms spontaneously by chemisorption, creating an organized, closely-packed group of long-chain organic molecules (see Figure 1). A SAM is typically formed by immersing an appropriate substrate into a solution of an active surfactant in an organic solvent, or by exposing the substrate to the vapor of the reactive species. The final structure is at or near thermodynamic equilibrium, so it tends to form spontaneously and to reject defects. [1] The interfacial properties of a SAM are largely determined by the chemical properties of the functional group at the end of the molecular chain. Chemisorption of an alkanethiol ($\text{CH}_3(\text{CH}_2)_n\text{SH}$) on gold surfaces yields an alkanethiolate ($\text{CH}_3(\text{CH}_2)_n\text{S}^-$) SAM. Formation of alkanethiolates on gold during microcontact printing can occur in a matter of seconds. This ability to form ordered structures rapidly is one of the advantages of microcontact printing. Most of the work to date has been done on gold because it can be handled in ambient conditions without forming an oxide.

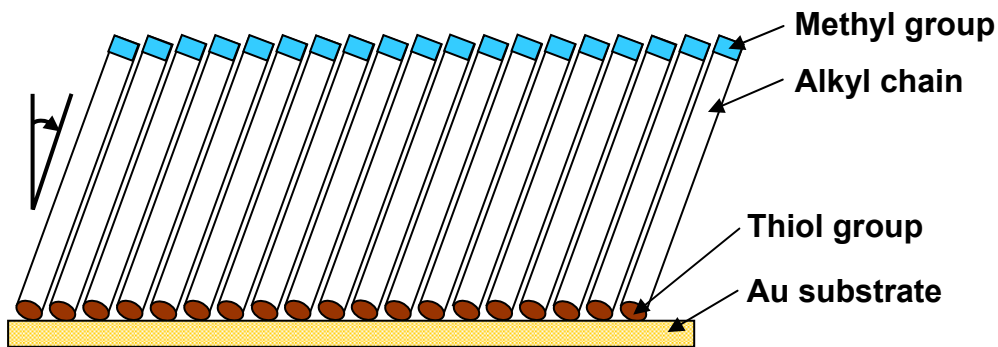


Figure 1. Diagram of self-assembled alkanethiolate monolayer.

Microcontact printing begins with a 2-D design which is transferred to a master by photolithography. A schematic of the microcontact-printing process on a flat substrate may be seen in Figure 2. An elastomeric stamp is made from the master; the stamp can be used to transfer the design to either a 2-D (flat) substrate or a 3-D substrate such as a cylinder. Once a master has been fabricated, multiple stamps can be made without further access to photolithographic facilities. In addition, a stamp can be used numerous times without a reduction in performance. After a SAM has been transferred to a metal (typically gold) film that has been deposited on a substrate, the substrate is immersed in a

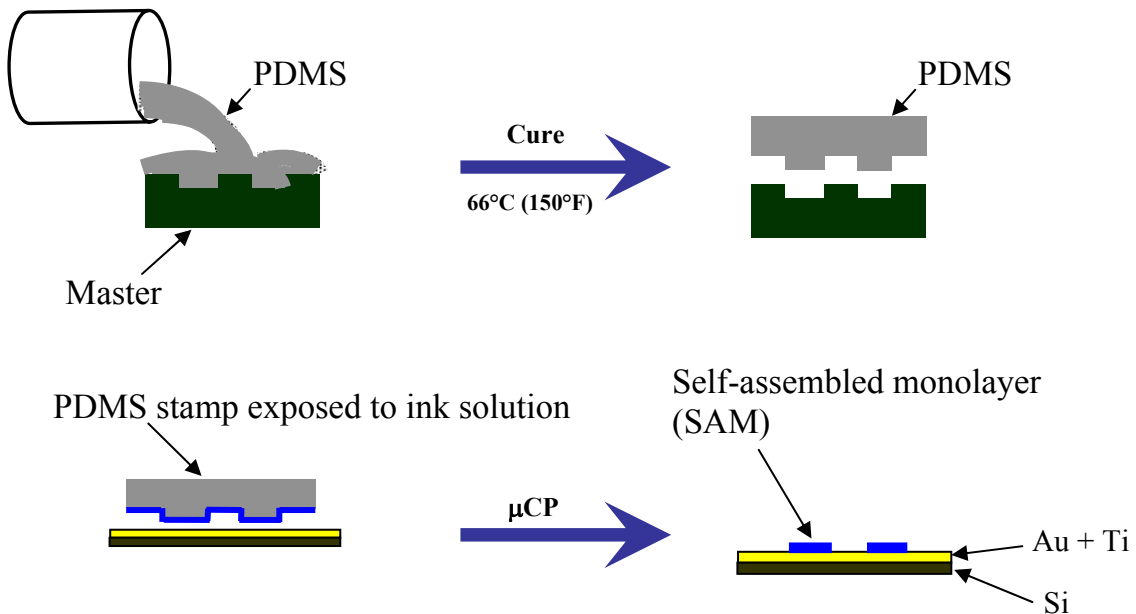


Figure 2. Procedure for microcontact printing (μ CP) on a flat substrate.

suitable wet etchant. The SAM acts as an etch resist during the wet etching, resulting in spatially-selective removal of the metal in areas not covered by the SAM. This produces a patterned metal film. Electroplating is often used to build up the thickness of the metal to make the final part more robust. Selective wet etching and electroplating of a patterned cylindrical part can produce a freestanding 3-D microcomponent.

In this report, we discuss the factors of microcontact printing and subsequent processing which affect the quality of the final product, and present some examples of patterns printed on 2-D and 3-D substrates. In addition, we discuss the differences between wet inking and contact inking.

Background: Microcontact Printing Has Been Used in a Wide Variety of Applications for both 2-D and 3-D Substrates

Many groups have successfully transferred a wide variety of patterns to both 2-D [2-17] and 3-D [3, 7, 8, 18-27] substrates using microcontact printing. Some innovative 2-D applications resulted in a variety of end uses. Kumar et al. [9] used microcontact printing and subsequent processing to produce a microelectrode array; the line width of the electrode was 2.5 μm , and the width of the space between electrodes was 1 μm . Huck et al. [6] printed a SAM which acted as a seed layer for building up patterned films of polymer multilayers; the features of the pattern were in the range of 1 to 10 μm . These patterned multilayer films provided improved etch resistance compared with a SAM by itself. Li et al. [28] produced an array of 100-nm-diameter cobalt dots on a silicon wafer for magnetic applications. The original structure was a silicon wafer first coated with polymethylmethacrylate (PMMA), then with titanium (as an adhesion layer) and finally with gold. After microcontact printing and selective wet etching of the gold, reactive ion etching of the titanium and PMMA was conducted. The remaining structures were used for lift-off of cobalt. Kumar et al. [29] patterned an array of microlenses by directing the flow of a UV-cured polyurethane on a surface patterned with hydrophobic and hydrophilic regions.

Several groups have used microcontact printing to create patterned surfaces of mixed SAMs that are suitable for biomedical applications such as biosensors. Mixed SAMs are SAMs with different functional groups on the exposed ends of the molecules. One way to produce a mixed alkanethiolate SAM is to immerse the substrate in a solution containing a mixture of alkanethiols for several hours [30, 31]. Another popular method of creating mixed SAMs is to print the first SAM and then immerse the patterned substrate in a solution of the second SAM, which covers the unprinted areas [29].

In many biological applications, a technique is needed to direct specific adsorption of a protein or cell onto a substrate; the entity of interest is often immersed in a solution containing a mixture of biomolecules. A common goal is to develop a method that can direct the attachment, spreading, and biological response of proteins or cells to a particular surface. Lahiri et al. [30] printed ligands on a gold surface covered with a

mixture of reactive alkanethiolate SAMs. This type of patterned surface can prevent nonspecific adsorption of proteins. In order to get the hydrophilic solution of ligands to wet the surface of the hydrophobic PDMS stamp, they oxidized the stamp by exposing it to plasma in air for one minute. The plasma treatment oxidizes the Si-CH₃ groups and generates Si-OH groups [32].

Ostuni et al. [31] studied the interaction of both proteins and cells with mixed alkanethiolate SAMs on gold and silver. By varying the functional groups of the alkanethiols, they were able to observe the effect of structure and polarity on the adsorption of proteins. Printing SAMs with different functional groups provided a way to monitor specific interactions of the desired protein by minimizing the background of nonspecific protein adsorption. In additional experiments, they used microcontact printing to make hydrophobic islands of different shapes on a gold substrate. They coated these islands with extracellular matrix proteins, which promote adhesion of certain mammalian cells. The resulting patterned surface directed the cells to adhere only to the protein-coated islands, thereby creating a way to pattern the attachment of cells. In general, mammalian cells need to adhere to a surface in order to grow. They were able to study the effects of the chemical character and topology of the surface on the cellular metabolism of mammalian cells. Kumar et al. [29] used a similar approach to pattern the attachment of mammalian cells to islands of protein-covered hydrophobic SAMs. The underlying substrate controlled the spreading of the cells.

Another area applicable to biosensors is patterned lipid bilayers. A lipid bilayer on a solid support such as a glass substrate is essentially a fluid resting on a thin (10-20 Å) layer of water. The purpose of patterning lipid bilayers is to provide barriers to lateral diffusion. This restricts the mobility of the lipids to the patterned areas, which makes it possible to fill the bare regions with other biomolecules such as proteins. Hovis et al. [33] patterned a lipid bilayer by blotting a surface covered with the bilayer structure. This selectively removed the lipid bilayer in the areas where the stamp touched the surface. They used a PDMS stamp to do the blotting, which was done under water. They used a weight on the stamp during the blotting to keep it from floating. The blotting took about 10 minutes. Once the lipid bilayer was selectively removed, the remaining material expanded slightly but then stopped, leaving bounded fluid regions of lipid bilayers. The patterned lipid bilayer was stable under water for at least one week. They were able to transfer the delicate bilayer that was lifted by the stamp to a new substrate. They were also able to stamp a lipid bilayer directly onto a glass substrate using a PDMS stamp treated with oxygen plasma to make it hydrophilic.

Yan et al. [32] covalently attached thin films of polyethylene imine to reactive alkanethiolate SAMs on gold and silver using microcontact printing. They exposed a PDMS stamp to oxygen plasma (10-second exposure at 0.2 Torr) to make the surface hydrophilic prior to inking. The patterned polyethylene imine films, once attached, provided a new reactive surface that could be modified through chemical reactions with a variety of functional groups.

There have been several inventive applications of microcontact printing to create 3-D structures. Rogers et al. [25] produced both single- and multiple-helical microcoils with printed wires that were 125 to 150 μm wide. They characterized the microcoils as components of microelectromagnets and microinductors. Jackman et al. [19] fabricated a concentric cylindrical microtransformer using microcontact printing and subsequent processing. The O.D. of the inner coil was 135 μm and that of the outer coil was 350 μm . An 80- μm -diameter ferromagnetic wire was threaded through the bore of the inner coil. The microtransformer performed very well at frequencies between 1 kHz and 20 kHz. At higher frequencies, a decrease in the permeability of the ferromagnetic core material limited the performance of the microtransformer; the performance could be optimized by trying different core materials. Rogers et al. [23] fabricated microcoils of 70- μm -wide printed wires on glass capillaries to use in high-resolution ^1H -NMR spectroscopy of nanoliter-size samples. After electroplating, strips of the wire were peeled back from the ends and used to connect the microcoil to the NMR data-acquisition circuit. The printed microcoils were constructed to replace the conventional 5-mm spinning tube probes.

Rogers et al. [24] printed copper bands on the surface of a 125- μm -O.D. optical fiber to create an amplitude photomask. They carefully rolled an optical fiber over a stamp inked with palladium colloids using a micromanipulator. Electroless deposition of copper, which is catalyzed by the palladium, generated a series of opaque copper bands bonded to the surface of the fiber. Exposure of this patterned fiber to UV light produced an in-fiber grating (a grating in the core of the fiber). They were able to expose the fibers to UV light for long periods with minimal interference from optical and mechanical instabilities.

Jackman et al. [20] formed 3-D structures by printing intricate designs on capillaries which, after subsequent processing and application of uniaxial strain, became complex structures such as free-standing hollow cubes. In addition, they fabricated microchains by transferring a half-links design to each of two silver-coated glass capillaries and then joining them. Electroplating the joined pair of capillaries produced interlocking links by electrochemically welding the two halves of each link together; in addition, it built up the thickness of the microlinks to make them more robust. Dissolving the underlying glass capillaries produced free-standing microchains. They used a different soft-lithographic method (not microcontact printing) to transfer the half-links pattern to the metallized capillaries. Deng et al. [34] used this same method to create a silver honeycomb pattern on a glass capillary. We discuss this alternative briefly in the Results section of this report.

Deng et al. [34] fabricated a microspring using microcontact printing to transfer a round spiral design onto a silver-coated silicon wafer. After selective wet etching, the patterned substrates were electroplated in a nickel bath. The line width of the spiral wire was approximately 10 μm and the thickness was 1-2 μm . Dissolving the underlying silicon caused the center of the spiral to rise above the rest of the part, creating a 3-D microspring. This type of microspring could be used as a sensing or actuating element in a microcomponent.

Rogers et al. [22] fabricated cylindrical microsprings that could be elastically stretched by more than 100%. In addition, they created a 3-D structure suitable for use as a coronary stent. They were able to expand this tubular structure by approximately 250% in diameter. The structure was expanded by inserting a balloon into its center and inflating the balloon, just as is done in an angioplasty procedure. The recoil (percent change in diameter) for the balloon as it was first inflated then deflated was $3.5 \pm 0.5\%$. Commercially available stents have recoils between 3% and 10%.

Brittain et al. [3] created “microorigami” using microcontact printing. They converted 2-D patterns to 3-D objects by folding sections of the patterned parts along hinges of pre-designed perforation lines. Separating the metal film from the glass substrate produced free-standing 3-D structures. By electroplating these delicate structures, they were able to weld the bent hinges into position, join separate pieces where needed, and build up the structural integrity of the final parts.

Current research has demonstrated that microcontact printing and subsequent processing can produce both 2-D and 3-D parts in a wide variety of applications. However, the studies typically produce a small number of parts since they are for proof of principle. To our knowledge, no group has studied the feasibility of manufacturing numerous copies of the same microcomponent using this approach.

Scope: Many Factors Affect the Integrity of the Final Part

There are numerous factors which affect the outcome of transferring a pattern to a thin metal film. High precision and repeatability are critical for the process to be suitable in a manufacturing environment. Much care must be taken in fabricating the master which is used to make the stamp. Any imperfections in the master will show up in the stamp, and subsequently in the printed pattern. It is essential to design the master to prevent the problems that can occur in the stamp due to the limp nature of the elastomer. In addition, it is important to minimize the uneven coverage of the SAM on the stamp and the pooling of ink solution in crevices or channels on the stamp during the inking process. If drops of solution are left on the stamp after the inking process, this results in solid spots in the final pattern. The diffusion of the ink solution to unpatterned areas of the stamp should be minimized, as well as the presence of debris in the ink solution. These factors can all diminish the quality of the final pattern.

Achieving accurate transfer of an intricate pattern without distortion is substantially more difficult with an elastomer than with a rigid material. If the aspect ratio (height/width) of the elastomeric features is too high (greater than 2), they can collapse onto each other (see Figure 3A), causing defects in the printed pattern. Delamarche et al. [35] recommend an aspect ratio between 0.3 and 0.6. Sagging can occur for patterns with features that are widely separated (see Figure 3B). Microcontact printing is not a suitable method for printing designs in which the features are widely separated.

Sylgard 184 silicone elastomer is the popular choice for the stamp material, and it works very well for many applications. Since it is an elastomer, it conforms to the surface of the substrate. Its low surface energy makes it self-releasing, which is a desirable property for the stamp. A Sylgard 184 stamp can be used multiple times without incurring damage. However, it is important to check the stamp periodically for tears, holes, or embedded debris. The presence of contaminants and defects in the stamp can cause debris or holes in the monolayer.

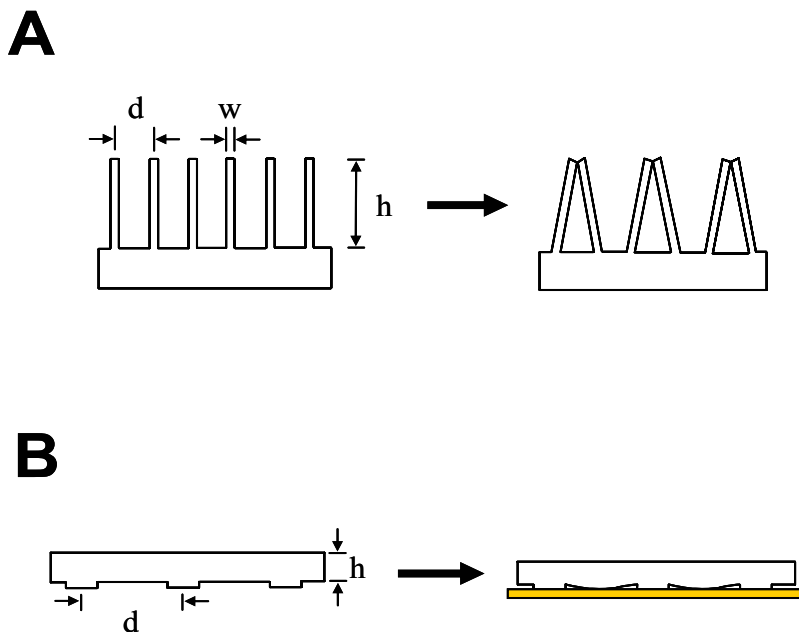


Figure 3. Problems from using incorrect aspect ratios (h/w) in designing a stamp. A. Collapse of features (h/w is too high). B. Sagging of recessed areas of stamp onto substrate (d/h is too high).

The optimum thickness of the stamp depends on the size of the features. If the stamp is too thin, it may have trouble attaining conformal contact with the substrate. In addition, a thin stamp is susceptible to damage from handling. On the other hand, if the stamp is too thick, the weight of the stamp will cause the entire surface to conform to the substrate indiscriminately. This results in completely losing the contrast of the raised features.

It is important to choose a suitable alkanethiol for the ink solution. During the self-assembly process, strong interactions between the alkanethiolate molecules and the substrate result in an apparent pinning of the head group to a specific site on the surface through a chemical bond. As the alkyl chain becomes longer, the assembly becomes more ordered, the organization being driven by van der Waals attractive forces between

adjacent chains. The chemisorption process is exothermic, releasing 40-45 kcal/mol for thiulates on gold. [36] As a result of the exothermic interactions between the head groups and the substrate, the molecules try to occupy every available binding site on the surface; in doing this, they push together molecules that have already adsorbed onto the surface. It is this spontaneous molecular adsorption that brings the molecules close enough to allow the short-range van der Waals forces to direct the assembly.

An alkanethiol must have eleven or more carbon atoms in its alkyl chain ($n \geq 11$ in $\text{CH}_3(\text{CH}_2)_n\text{SH}$) for a SAM to form a closely-packed, ordered structure. Shorter-chain alkanethiols do not provide adequate protection of the underlying substrate during wet etching [37]. Their ability to resist the etchant decreases as the chain gets shorter. In general, methyl-terminated alkanethiolates provide the greatest resistance to etching, while those terminated in polar functional groups provide less resistance [10]. The most widely-used alkanethiol for microcontact printing is n-hexadecyl mercaptan or 1-hexadecanethiol (HDT). The chemical structure of HDT is $\text{CH}_3(\text{CH}_2)_{15}\text{SH}$. The thickness of HDT on gold is approximately 20 Å, as estimated by ellipsometry [38]. Grazing-angle FTIR data suggest a tilt angle of 20° to 35° from the surface normal [39]. HDT is the longest-chain alkanethiol that is liquid at room temperature.

The concentration of the alkanethiol in the ink solution is critical to the success of the printing process. Larsen et al. [40] examined the structures of dodecanethiol ($\text{CH}_3(\text{CH}_2)_{11}\text{SH}$) SAMs formed by microcontact printing and compared them with SAMs formed in a solution of dodecanethiol in ethanol. They found that the SAMs formed by microcontact-printing have the same organization and distribution of defects as SAMs formed in solution for dodecanethiol concentrations greater than 10 mM. They found that the integrity of the SAM formed by microcontact-printing depends on the concentration of the ink solution used to ink the stamp. On the other hand, it is independent of the time that the stamp is in contact with the gold surface for contact times greater than 0.3 seconds. They typically used a contact time of 10 seconds. They got similar results for contact times of 1-30 seconds. They chose dodecanethiol because it forms a thinner (~1.3 nm thick) SAM than HDT (~2 nm thick), while still forming an ordered monolayer on gold. This smaller thickness allowed them to do STM studies at tunneling currents of 1 to 10 picoamperes.

Other factors affecting the quality of the ink solution are the choice of solvent, the possible presence of water, the possible oxidation of HDT, the age of the solution, and the presence of residue or debris that could be transferred to the stamp during the inking process. While a clean room is not required for this work, the working area must be kept clean enough to avoid contaminants and defects in the SAMs.

Microcontact printing has been done on gold, silver, and copper using ink solutions with concentrations of HDT in ethanol from 0.1 mM to 10 mM [7, 9-12, 34, 35, 41, 42]. Xia et al. [42] used a 2 mM solution of HDT in ethanol to create a variety of test patterns in gold, silver, and copper; the selectivity and edge resolution were excellent for both silver and gold, but were much poorer for copper. We tried different concentrations of HDT in ethanol for printing patterns on gold. Concentrations above 16 mM produced poorly-

defined patterns. A 5 mM solution worked well when transferring patterns to silver [43]. We typically used 8 mM solutions of HDT in ethanol to transfer patterns to gold.

There is a delicate balance between achieving defect-free protection of the substrate and favoring the transport of excess HDT molecules. For example, if an ink solution is weak, stray diffusion is not a problem but the SAM is not completely formed. On the other hand, if a solution is too concentrated, more HDT molecules will diffuse away from the stamped area. The contact time and the concentration both influence this. Highly concentrated solutions can cause blurred areas and severe broadening of feature widths, which are apparent after wet etching; this can occur even at short contact times [4].

A wide range of contact times has been used to transfer SAMs of HDT onto gold. Contact times as short as 5 seconds or less have been reported in the literature [2, 7, 34, 35, 40, 42, 44]. According to Xia and Whitesides [1], a typical contact time for a stamp wet-inked with a 2 mM solution of HDT in ethanol is 10 to 20 seconds.

There are four methods commonly used to apply the ink solution to the stamp: 1) covering the surface of the stamp with the ink solution (wet inking), 2) immersing a cotton swab in the ink solution and then brushing it across the surface of the stamp, 3) placing the stamp on a presoaked lint-free paper or cloth, and 4) placing the stamp on a presoaked PDMS inking pad (contact inking). Since using a cotton swab can damage the stamp, we did not use this method. Preliminary tests gave mixed results when using a presoaked lint-free cloth as the inking pad; therefore, we did not pursue this method. In this work, we used both wet inking and contact inking.

Wet inking supplies the ink solution to the entire stamp surface (see Figure 4), not just to the features of interest. After wet inking of the stamp, it is best to remove the excess solution with dry nitrogen before the printing step. In this inking method, the HDT molecules can disperse in many directions (see Figure 5). Diffusion of the HDT molecules can cause the etched design to have a mottled background of unetched gold or an enlargement of the desired features. There is a delicate balance between giving the stamp enough time on the substrate to fully form a SAM, and allowing time for the HDT molecules to diffuse to areas away from the regions of contact.

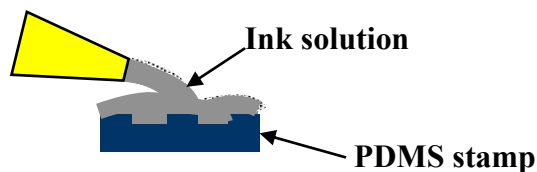


Figure 4. Wet inking of a stamp.

In contact inking, the stamp is placed in conformal contact (see Figure 6) with a flat, smooth (unpatterned) sheet of PDMS which is soaked in the ink solution for at least 12 hours prior to use. The presoaked PDMS sheet is referred to as the inking pad. The smoothness of the PDMS surface favors the formation of a void-free interface between of the stamp and the inking pad through which the transfer of HDT is possible. Contact inking has many advantages over wet inking. For example, the features of the patterned surface are not subjected to capillary forces. In wet inking, capillary forces are created from the wetting and dewetting of the ink solution on the surface. In addition, no drying of the surface is necessary after the contact-inking step, thereby preventing damage to delicate parts of the stamp. The only drying that is necessary is the drying of the presoaked inking pad prior to use. Another advantage of contact inking is the ability to produce stamps that can simultaneously print both large and small features. This is difficult to do when wet inking the stamp due to the stray diffusion of the HDT molecules to the gold surface. Contact inking results in excellent contrast of the etched pattern (see Figure 7).

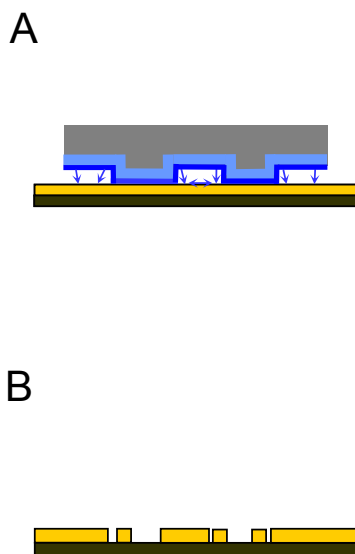


Figure 5. Diffusion of HDT molecules (shown by blue arrows) due to the wet-inking method. A. The ink solution is present in the cavities of a stamp as well as in the areas of contact. B. The stray HDT molecules can result in unwanted gold spots in the etched pattern.

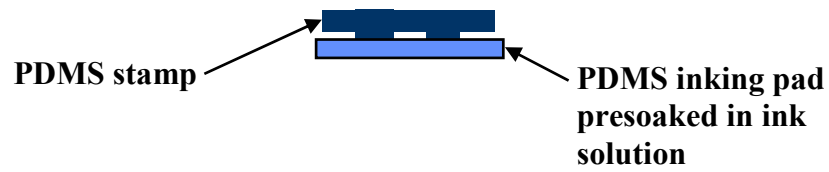
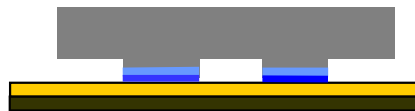


Figure 6. Contact inking of a stamp.

A



B



Figure 7. Contact inking produces a cleaner pattern transfer than wet inking. A. Stamp is inked only in places where it touches the substrate. B. The resulting etched pattern is free of unwanted gold spots.

Microcontact printing is essentially a dry process: no liquid should be present on the surface of the stamp as it makes contact with the substrate. The less volatile alkanethiol remains on the surface of the stamp, presumably in the gas phase, while the ethanol evaporates. However, there is some amount of alkanethiol that diffuses into the bulk of the stamp. The vapor-phase equilibration of the HDT in the bulk of the stamp allows the HDT to diffuse to the surface after each stamping has released the top layer of HDT molecules; this allows multiple stampings after just one inking. This is true for both wet inking and contact inking. The gold surface arrives at a limiting state where further adsorption of HDT molecules is inhibited by the layer already adsorbed onto the surface. Excess HDT remains on the stamp since an HDT SAM is not wetted by HDT. The monolayers remain relatively free of residues from the microcontact-printing process such as excess thiols, contaminants on the gold surface, or residues extracted from the PDMS stamp. This shows the ability of the covalent self-assembly process to minimize contaminants on the surface of the substrate.

The accuracy of transferring the design to the substrate is determined by the uniformity of force on the stamp and the contact time between the stamp and substrate. Too much force can cause distortion of the features or at worst, a solid strip of metal (with an absence of the pattern). Too little force results in pale spots or holes in the etched pattern. Uneven contact of the stamp with the substrate can lead to distorted or incomplete patterns. It is important to minimize shear forces from acting on the stamp during the printing step or when removing the stamp from the substrate. If the stamp rubs the surface, it will result in blurred areas of the pattern. If it skips over the surface during placement or removal, it will leave excess printed features. For printing capillaries, additional concerns include the alignment of the capillary on the stamp and the rate at which the capillary is rolled over the stamp. For example, improper alignment will cause the helical structure to be discontinuous when printing the microcoils pattern. If the capillary jumps over the stamp during the printing process, this will cause holes in the resulting pattern.

It is important to optimize the wet etching process so that it will selectively remove the gold film in a repeatable manner. If the thin-film deposition of a metal coating on a substrate does not produce approximately the same thickness for each part, then the etching process cannot be optimized. Any deviation in thickness requires a reevaluation of the etching time.

When a gold film is exposed to a solution containing cyanide (CN^-) ions and an oxidant such as oxygen or potassium ferricyanide, the gold dissolves [29]. The SAM acts as a physical barrier to mass transport, limiting access of the etchant to the underlying gold film. HDT was used as the etch resist in our work; it provided excellent protection of the gold during etching in a cyanide solution. The HDT molecules essentially exclude the cyanide ions so that they cannot penetrate through the SAM to the gold surface. However, if the stamping does not achieve fully conformal contact with the substrate during the printing process, then etch pits can result from incomplete coverage of the substrate with the SAM.

In selective wet etching, the ratio of components in an etchant solution must be optimized so that it can selectively remove the unprinted gold in a reasonable amount of time. An incorrect ratio can result in no selectivity in the removal of the gold film. Depending on the components in the etchant, it can also produce a discoloration in the metal surface. In addition, the etching time has to be monitored closely. The metal cannot be selectively removed if it's taken out of the etchant too soon. On the other hand, the entire metal film is removed (leaving no pattern) if left in the etchant too long.

The length of time between microcontact printing and etching is important, since the HDT oxidizes over time and disappears in a fairly short period of time (10-14 days). The oxidation of thiols on exposure to air is well known; the occurrence is sensitive to both UV irradiation and the presence of metal ions. Huang et al. [45] detected alkanesulfonate species (RSO_3^-) as photooxidation products of straight-chain alkanethiols after several days in air. They propose that the photooxidation of the alkanethiol SAMs occurs via UV excitation of the electrons in the gold substrate, followed by oxidation of the alkanethiolate species (RS^-). The lack of stability of alkanethiol SAMs in air is likely due to the covalent nature of the sulfur-gold bond.

The structural integrity of the final parts depends on the efficiency of the electroplating process. Discussion of the electroplating process is beyond the scope of this report.

Experimental: Several Tasks Are Required to Produce a Part with Microcontact Printing

Thin silver, copper, and gold films (100 to 200 nm) were deposited by electron-beam evaporation on silicon wafers, glass slides, and glass capillaries of 1.6 to 1.8 mm outer diameter. A thin film (~10 nm) of titanium was deposited on the silver and gold parts to promote adhesion; likewise, an adhesion layer of ~10 nm chromium was deposited on the copper parts. A special fixture (shown in Figure 8) was designed to deposit coatings on the glass capillaries. It was later modified to accommodate more capillaries.

The masters were made of SU-8 negative, near-UV photoresist (MicroChem Corporation, Newton, MA) patterned by photolithography on micropolished silicon wafers of (100) orientation (Silicon Sense, Nashua, NH). The SU-8 photoresist is formulated from a multifunctional bisphenol-A Novolac-based epoxy resin with a photoacid generator as the curing agent [46]. Figure 9 shows a general outline of the photolithography process. Before beginning the process, the wafers were cleaned with acetone and rinsed with deionized water before being etched in piranha solution for about 8 minutes. Piranha solution consists of a 1:1 mixture (by volume) of H_2SO_4 and 30% aqueous solution of H_2O_2 . The piranha solution was rinsed off in an overflow rinse of deionized water for 5 minutes. After being etched, the wafers were dried in nitrogen and baked on a 200°C hotplate for at least 5 minutes.

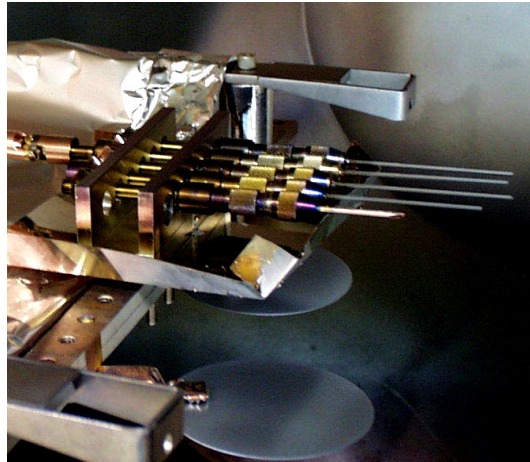


Figure 8. Special fixture for thin-film deposition of coatings on glass capillaries.

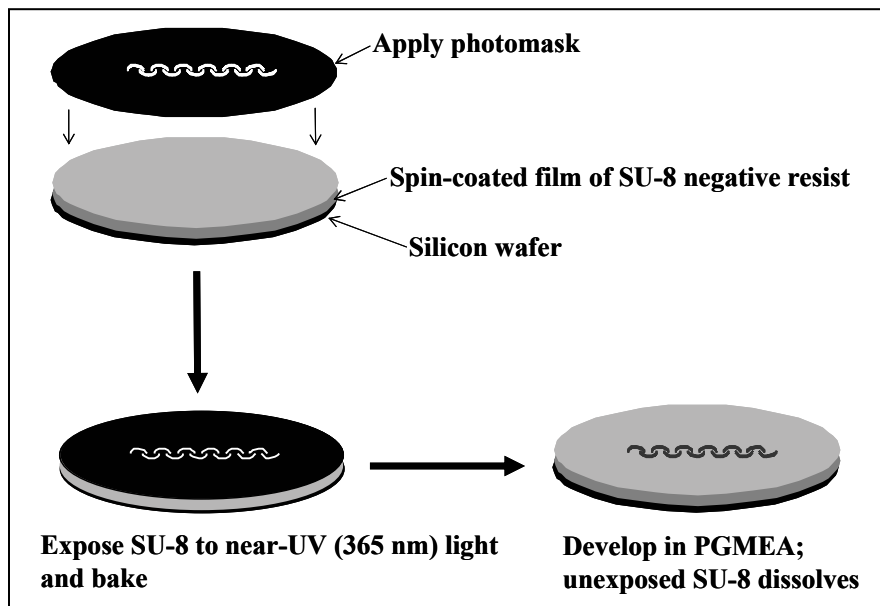


Figure 9. Procedure for creating SU-8 master using photolithography.

We dispensed 3 to 4 ml of the SU-8 25 epoxy photoresist directly onto the wafer and let it rest for several minutes before the spin-coating step. The vacuum chuck on the spin-coater was leveled prior to use with a Mititoyo digital level. Each wafer was centered by hand to minimize the occurrence of wobble during the spin-coating operation. We spin-coated the SU-8 25 for approximately 60 seconds at 690 rpm. The SU-8 25 contains gamma-butyrolactone (GBL) as the solvent. A well-known disadvantage of the GBL-based SU-8 formulations is the poor wetting of low-surface-energy substrates such as silicon; this can result in non-uniform thickness of the coating. We had repeated problems with dewetting of the SU-8 25 from the surface of the silicon wafer. We let the SU-8 25 samples sit for several minutes to several hours before continuing with the procedure to maximize the time allowed for the photoresist to spread out and for air bubbles to rise to the surface. Prebaking the wafers at 160°C for at least 30 minutes prior to use seemed to help minimize the dewetting. We poured the SU-8 25 directly out of the bottle onto the wafer because this produced fewer air bubbles and less dewetting than when it was dispensed by a syringe.

We primed some silicon wafers with hexamethyldisilazane (HMDS) to increase the wettability of the SU-8. We spin-coated the HMDS on clean, dry wafers for 30 seconds at 4000 rpm. We tried this for a couple of different SU-8 formulations and it worked very well. Vapor deposition of HMDS is also used to prime silicon wafers.

Each photoresist-coated wafer was soft-baked on a hot plate for 10 minutes at 65°C and then 25 minutes at 95°C to remove all the solvent from the photoresist. Each wafer was placed on a thin ceramic plate for the soft-bake steps. The hot plates used in this work were Cole Parmer digital hot plates, and they were leveled prior to use with a Mititoyo digital level. The temperatures of the hot plates were monitored using a Type K (NiCr-NiAl) thermocouple (Omega Engineering Inc.).

The photoresist coating was exposed through a photomask to a near-UV (365-nm) light source (Hybralign Series 500 by Optical Associates, Inc.) for 29 seconds to accumulate a total dose of 430 mJ/cm². The light intensity and timer accuracy were calibrated before use. The pattern for the photomask was designed using Freehand 9 (Macromedia, Inc.) software. Subia Corporation (Albuquerque, NM) printed each pattern on acetate film using an imagesetter. Quartz plates (Quartz Plus, Inc., Brookline, NH) were placed on the photomask to ensure contact between the photomask and the photoresist. The post-exposure bake was done in two steps, first at 75°C for 10 minutes, then at 95°C for 15 minutes.

The SU-8 master was developed by immersion in propylene glycol monomethyl ether acetate (PGMEA) with slight agitation for several minutes. The part was checked periodically to see if it needed more time in the PGMEA. When it was completely developed, it was rinsed with PGMEA, spray-washed with isopropanol, and then rinsed in deionized water. It was blown dry with nitrogen.

The fabrication of the SU-8 masters was done in a Class 1000 cleanroom. The thickness of the SU-8 25 photoresist in the final part was approximately 60 μm . The feature sizes were 100 to 150 μm for the microcoils master. We designed our masters to produce features with an aspect ratio (h/w in Figure 3) of 0.4 to 0.6, which is in the range recommended by Delamarche et al. [35].

To make a master using a chrome photomask with features as small as 1 μm , we used the SU-8 2002 negative, near-UV epoxy photoresist, which gives a final thickness of 2 to 5 μm [47]. This formulation uses cyclopentanone as the solvent, instead of GBL. The cyclopentanone has much better wetting of silicon than GBL. We used a procedure similar to the one described above to prepare the silicon wafers for photolithography. We dispensed 3 to 4 ml of the SU-8 2002 photoresist directly onto the wafer using a digital pipette. We spin-coated the SU-8 2002 for approximately 30 seconds at 1500 rpm. Each wafer was primed with HMDS and then coated with SU-8 2002 before proceeding to the next wafer. Each photoresist-coated wafer was soft-baked on a thin ceramic plate on a hot plate for 1 minute at 60°C, 2 minutes at 95°C, and then 15 seconds at 60°C. The part was exposed through a photomask to a near-UV (365-nm) source for 8.2 seconds at 123 mJ/cm^2 . The post-exposure bake for the SU-8 2002 was done at 60°C for 1 minute, at 95°C for 1 minute, and then at 60°C for 15 seconds. The SU-8 2002 master was developed by immersion in PGMEA with slight agitation for several minutes. Some places on the SU-8 2002 master showed a loss in adhesion for the finer features. The SU-8 masters were post-cured for approximately 16 hours at 66°C.

Parts A and B of the Sylgard 184 silicone (Dow Corning Corporation, Midland, MI) were mixed in a 10:1 ratio by weight. Sylgard 184 is formulated from a vinyl-terminated prepolymer linked through a short hydrosilane cross-linking agent using a platinum complex as the catalyst [13]. After mixing for at least 2 minutes, the Sylgard 184 was placed in a vacuum chamber and exposed to a vacuum of approximately 584 Torr and held under vacuum for at least 1 minute after the foam rise collapsed. Then it was poured over the master to form the stamp. The masters were silanized by vapor deposition of (tridecafluoro-1,1,2,2-tetrahydrooctyl) trichlorosilane (Gelest, Inc., Tullytown, PA) under house vacuum for 4 to 8 hours so that the Sylgard 184 would release from the master after cure. After sitting at room temperature for at least 30 minutes, the Sylgard 184 was cured at 66°C for approximately 16 hours. After cooling to room temperature, the stamp was carefully peeled from the master. Sylgard 184 has a linear cure shrinkage of less than 2% [13].

The thickness of our stamps ranged from 2 to 5 mm. We found the 5-mm thickness to be the upper limit of usefulness. Its weight can cause the whole surface of the stamp to conform to the surface of the substrate if the features did not provide sufficient stand-off; this makes the raised features indistinguishable from the rest of the stamp.

We used n-hexadecyl mercaptan or 1-hexadecanethiol (HDT) in ethanol for the ink solution. The HDT was used as received from Acros Organics USA (Morris Plains, NJ) with no further purification. Pure 200-proof, anhydrous ethanol was purchased from

Aaper Alcohol and Chemical Company (Shelbyville, KY). Anhydrous diethyl ether was used as received from Fisher Scientific (Pittsburgh, PA).

The inked stamps were used within 15 seconds after inking for both wet inking and contact inking. For wet inking, we covered the entire surface of the stamp with the HDT/ethanol solution for 1 to 2 minutes, using a new pipette each time. The excess ink solution was blown off the surface of the stamp with nitrogen prior to the printing step.

For contact inking, the inking pad was soaked in the HDT/ethanol solution for at least 12 hours prior to use in a sealed 20-ml vial. We used a flat (unpatterned) piece of Sylgard 184 as the inking pad. The stamp was placed on top of the presoaked inking pad (without applying pressure) for approximately 45 seconds. Conformal contact of the patterned face of the stamp and the inking pad for at least 30 seconds allowed transfer of the HDT molecules to the raised features of the stamp. Longer contact-inking times produced blurred areas in the resulting pattern due to the stray diffusion of HDT molecules. Libioulle et al. recommend a contact-inking time of 40 seconds and a printing time of 30 seconds [11]. We used a printing time of at least 1 minute for both wet inking and contact inking.

For transferring a pattern to the capillaries, we used a computer-controlled micromanipulator (Aerotech, Inc., Pittsburgh, PA) with a 3-stage positioning system which included a rotary positioning stage. A CCD camera with macro capability was mounted above the micromanipulator (see Figure 10). A special fixture was constructed to hold each end of the capillary while allowing it to roll over the stamp (see Figure 11). Thin cylindrical boots of Dow Corning HS II silicone (Dow Corning Corporation, Midland, MI) were made to hold the capillary ends securely in the fixture; these compensated for differences in diameter of the capillaries.

After printing a substrate, the part was immediately immersed in an appropriate etch solution. The wet etching was done at room temperature. The Pyrex beaker containing the etch solution was open to the ambient air. For the gold etchant, we used a mixture of 0.1 M potassium cyanide (KCN) and 0.001 M potassium ferricyanide ($K_3Fe(CN)_6$) as recommended by Kumar et al. [10]. We found that a 1:2 ratio by volume of potassium cyanide to potassium ferricyanide worked best. Using a solution more concentrated in cyanide caused the gold surface to look scorched after etching. Vigorous stirring with a magnetic stir bar during the etching produced a much cleaner pattern transfer and took less time than without stirring. The bare (unpatterned) regions of the gold were removed in 10 to 15 minutes.



Figure 10. Micromanipulator used for printing capillaries.

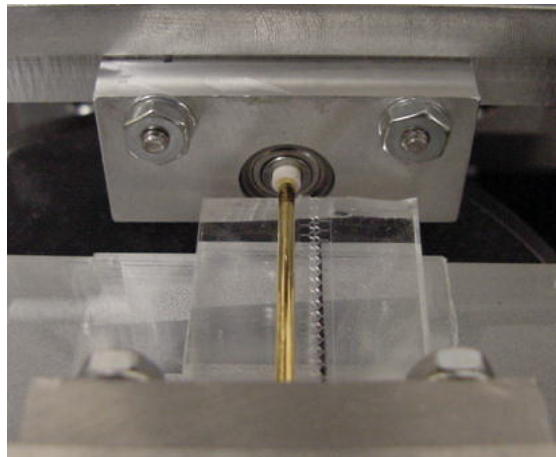


Figure 11. Fixture for holding capillary in micromanipulator.

We used the following mixture (in a 1:1:1 ratio by weight) to etch silver as recommended by Jackman et al. [20]: 0.001 M potassium ferrocyanide ($K_4Fe(CN)_6$), 0.01 M potassium ferricyanide ($K_3Fe(CN)_6$), and 0.1 M sodium thiosulfate ($Na_2S_2O_3$). It took approximately 2 minutes to selectively etch a 200-nm-thick film of silver on a silicon wafer (with 10 nm titanium as the adhesion layer). We used Tra-Con 2902 silver epoxy (Tra-Con, Inc., Bedford, MA) to adhere two capillaries patterned with the half-links design. We also used this silver epoxy to attach wires to the ends of the microcoils for electroplating.

We successfully printed patterns on copper using an 8 mM HDT/ethanol solution, but we were unable to selectively etch the copper patterns. It was interesting to see that a pattern could be seen on the copper surface before etching, and it became more pronounced over time. This is not the case with gold – the pattern cannot be seen until after etching. Moffat et al. [12] transferred patterns to copper using 5 mM HDT in ethanol; they observed that the copper patterns became visible over time, presumably due to the differences in oxidation rates for the bare and SAM-covered surfaces. We tried etching a copper film of 200 nm thickness (with 10 nm chromium as the adhesion layer) using a mixture of 20 mM sulfuric acid (H_2SO_4) and 0.15 mM chromic (VI) oxide (CrO_3), but were unable to get good resolution of the copper pattern. Next, we tried etching the copper with a mixture of 12 mM ferric chloride ($FeCl_3$) and 1M hydrochloric acid (HCl) as recommended by Xia et al. [16] using different proportions of $FeCl_3$ to HCl. For each case, the samples looked tarnished and discolored. While the printed pattern was still visible after etching, the etchant did not cleanly remove the copper in the unpatterned areas. Longer etching times simply removed the copper everywhere, including the printed areas.

Results: Contact Inking is Better than Wet Inking for Transferring Patterns with Fine Features

We conducted a screening study to identify candidate materials to use for the stamp. The silicones used in the study were: HS-II RTV, Silastic S RTV, Sylgard 184, and Silastic J RTV (all from Dow Corning Corporation, Midland, MI). Three different formulations of Conathane EN-25 polyurethane (from the Conap line of Cytec Industries Inc., Olean, NY) were used: EN-25/100:140, EN-25/100:126, and EN-25/100:80. Table 1 shows the materials we looked at and their hardness values.

We cut small squares of each material; a typical sample size was 8 mm wide, 11 mm long, and 3 mm thick. A dilute (~8 mM) solution of (tridecafluoro-1,1,2,2-tetrahydrooctyl) trichlorosilane in toluene was used to ink the samples; each sample was placed in the solution for approximately 1 minute and then allowed to dry until no liquid was visible on the surface of the stamp. Each inked sample was then brought into contact with the surface of a glass slide. All of the materials seemed to transfer silane to the glass slides; drops of water deposited on a slide moved away from the stamped (hydrophobic) areas. However, we did not use these materials to stamp metal surfaces in preparation for selective wet etching, so we are uncertain if they can effectively transfer a SAM to act as an etch resist.

Table 1. Candidate Materials for Elastomeric Stamp.

| Name of Material | Mix ratio (Resin:Curative) | Hardness (Shore A) |
|------------------------------|-------------------------------|-----------------------|
| HS-II RTV silicone | 10:1 | 20 |
| Silastic S RTV silicone | 10:1 | 24 |
| Sylgard 184 silicone | 10:1 | 45 |
| Silastic J RTV silicone | 10:1 | 55 |
| Conathane EN-25 polyurethane | 10:14 | 25 |
| Conathane EN-25 polyurethane | 10:12.6 | 34 |
| Conathane EN-25 polyurethane | 10:8 | 58 |

We decided to proceed with Sylgard 184, since this is the stamp material most often cited in the literature for microcontact printing. Sylgard 184 has a Young's modulus of approximately 1 MPa [4] and a compressive modulus of about 2 MPa [13]. Since the Sylgard 184 performed well in our applications, there was no need to use another material. For example, the Sylgard 184 effectively replicated a parabolic structure made by focused-ion-beam (FIB) sputtering in a silicon master (see Figure 12). The Sylgard 184 replica was 22.9 μm long, which is close to the length of the parabolic structure (20 μm). The depth of the FIB structure was 2.75 μm ; the depth of the Sylgard 184 replica was slightly less at 1.84 μm .

Other solvents such as hexane, isooctane, and toluene have been used in HDT solutions, but the resulting printed designs had poor resolution [10]. To see the effect of different solvents on Sylgard 184, we placed rectangular pieces (average dimensions: 24.8 mm \times 7.9 mm \times 2.5 mm) in four 20-ml vials for 3 days. Each vial contained one piece of Sylgard 184 and was filled with a different solvent: 1) ethanol, 2) toluene, 3) chloroform, or 4) a mixture of 71% toluene and 29% chloroform. The ethanol-soaked sample gained approximately 4.7% of its original weight and its shape remained unchanged. Each dimension of this sample increased by only 2%. This result agrees with the findings of Delamarche et al. [4]. For each of the other three samples, the weight increased by more than twice the original weight. In addition, the shapes of these samples were noticeably bowed. The length and width of the toluene-soaked sample increased by 26%, the thickness by 27%. The length of the chloroform-soaked sample increased by 20%, the width by 18%, and the thickness by 13%. The toluene/chloroform mixture caused the length of the sample to increase by 18%, the width by 20%, and the thickness by 17%.

We used pure 200-proof, anhydrous ethanol to make our HDT solutions, since Sylgard 184 is only minimally distorted by it. Pure (not denatured) ethanol is the most popular selection in the literature [1, 9, 14, 28, 29]. In addition, we tried diethyl ether as suggested by Kumar et al. [9] as an alternative to the ethanol. The diethyl ether repeatedly produced blurred patterns for a wide range of HDT concentrations, so we did not continue its use. Initially, the stamp was inked by rubbing its surface with a cotton swab saturated with the ink solution. This method was abandoned once it was discovered that it was damaging the features of the stamp.

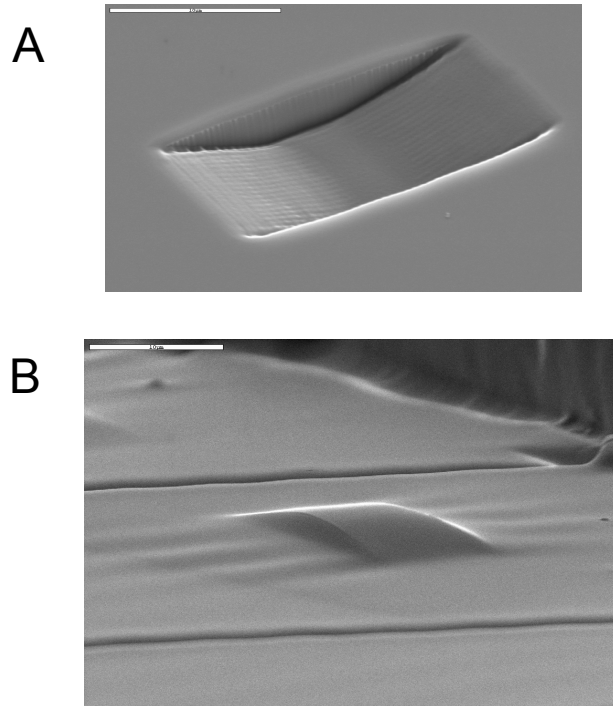


Figure 12. Replication of FIB structure with Sylgard 184.
A. Parabolic structure created by FIB in a silicon master.
B. Sylgard 184 replication.

We used a brass master (see Figure 13) to make a stamp (see Figure 14) for printing a thunderbird design on a gold-coated silicon wafer. This master was made with a 25- μm -diameter micro-end-mill tool fabricated by FIB milling. The surface roughness in the trenches that outline the thunderbird is less than 200 nm. The resulting stamp replicated (in reverse) the relief of the features on the master; that is, the raised features of the stamp (the outline of the thunderbird) correspond to the machined trenches of the master. It can be seen by comparing Figures 13 and 14 that Sylgard 184 did an excellent job of replicating the features of the brass master. Even the multitude of small scratches on the surface became part of the stamp. It is clear from this example that the quality of the master is critical to the integrity of the stamp, which affects the quality of the printed pattern.

We successfully transferred the thunderbird pattern to gold-coated silicon wafers using the wet-inking method. We were able to print complete SAMs even after the gold-coated wafers had been stored in the laboratory at ambient conditions for several days prior to use. It is widely known that freshly-deposited gold becomes contaminated with a thin ($\sim 1\text{-nm}$ -thick) layer of adsorbates such as atmospheric moisture within one day at ambient conditions. However, this adsorbed layer is readily displaced by an alkanethiolate SAM [4].

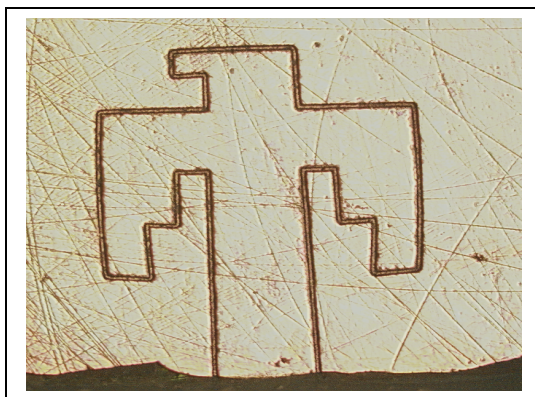


Figure 13. Brass master made with a 25- μm -diameter micro-end-mill tool fabricated by FIB milling.

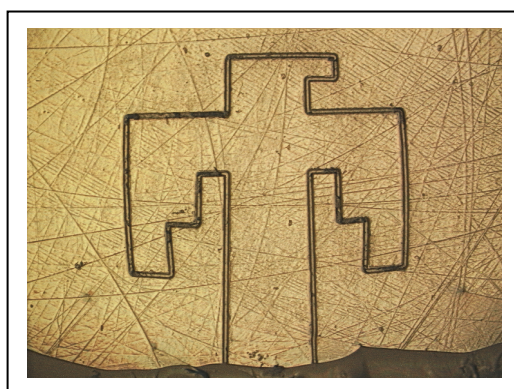


Figure 14. Sylgard 184 stamp made from brass master.

An image of the HDT SAM is shown in Figure 15. The 2-nm-thick monolayer is not thick enough to spatially resolve in the SEM. However, we were able to image the monolayer by capturing the difference in secondary-electron emissions from the monolayer and the gold. As a result of the SEM's electron beam interacting with the insulative HDT monolayer and causing a "charging" situation in the SEM, an insulator such as HDT can emit more secondary electrons than a conductor such as gold. This produces a contrast between the grounded conductor and the floating insulator. It is interesting to note that the holes in the printed monolayer (upper right-hand corner of the thunderbird in Figure 15) can be traced back to a defect in the stamp (upper left-hand corner in Figure 14) and subsequently to a defect in the brass master.

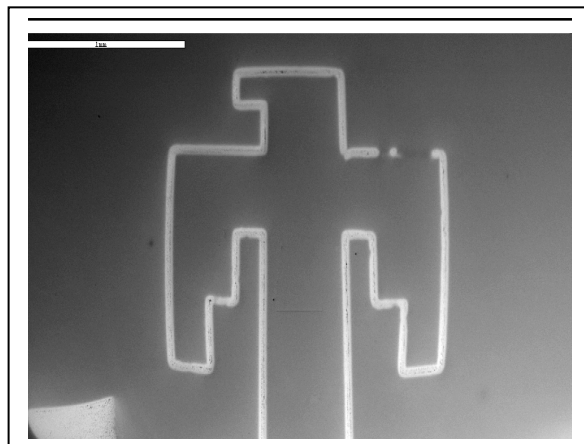


Figure 15. SEM image of HDT monolayer created by microcontact printing.

We got the best pattern transfer when we etched the samples the same day that we stamped them. When left in air at ambient conditions, the HDT SAMs disappeared after about two weeks. We stored both the pure HDT and the HDT solutions in the dark at room temperature.

We successfully transferred a variety of patterns to flat substrates of silver (see Figure 16) and gold (see Figure 17) using the wet-inking method. We cleaned the surface with ethanol prior to printing for some of the parts, but did not notice a difference between cleaned and as-received substrates. Both worked equally well.

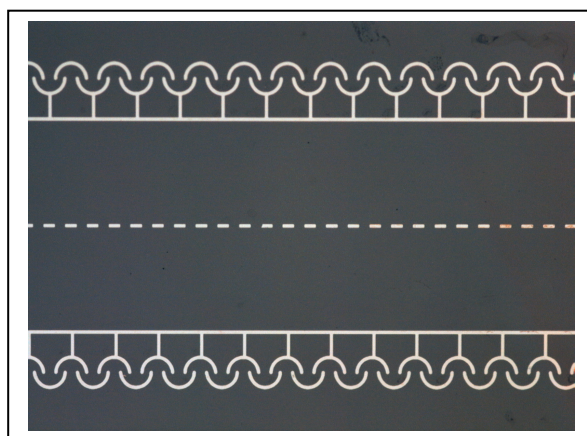


Figure 16. Two sets of the half-links pattern in silver on a silicon wafer. The line width is $\sim 100 \mu\text{m}$. The length of one half-link is $\sim 1 \text{ mm}$.



Figure 17. Examples of gold patterns on 2-D substrates. The line width is $\sim 100 \mu\text{m}$ for the half-links design and $\sim 225 \mu\text{m}$ for the parallel lines. The rectangular holes in the mesh design are $\sim 60 \mu\text{m}$ by $\sim 100 \mu\text{m}$.

The printing was performed with no force placed on the stamp; the weight of the stamp was enough to attain good conformal contact with the substrate. If it appeared that an area of the stamp was not conforming to the surface (possibly due to an uneven thickness of the stamp), the back of the stamp was tapped lightly with tweezers. The contact between the stamp and the substrate could be observed because the interface changed appearance as the area of contact spread under the weight of the stamp. During the printing step, efforts were taken to prevent shear forces from acting on the stamp as it was placed on the substrate and as it was removed.

The wet etching was done until the bare (unpatterned) gold was completely removed. We discovered that the selective wet etching of gold did not work for thicknesses greater than 150 nm. For samples coated with a 200-nm thickness of gold, the SAM was unable to protect the underlying gold for the extended etching time needed for this thicker layer. For our work, a gold thickness of approximately 100 nm was optimum.

Examination of the size and shape of the printed designs after wet etching provided a simple yet effective assessment of the accuracy of the pattern transfer. Although etching the metal film to examine the quality of the SAM is an indirect approach, it proved to be much easier than trying to find defects in the SAM by either SEM or AFM. We developed our procedures for microcontact printing and selective wet etching using flat substrates first, and then used the optimized processes on 3-D parts.

We attached wires to flat microcoils (see Figure 18) for electroplating operations. This process proved to be problematic. We were unable to solder wires onto the microcoils, since the heat of the soldering iron melted the gold and caused it to run. Silver epoxy was difficult to apply in small amounts due to its high viscosity. In addition, it did not have good adhesion to the gold, so wires often popped off during handling.

It is interesting to note that, even with numerous scratches on the etched gold patterns in Figure 18 (left-hand side), there was still sufficient electrical continuity for electroplating. We transferred the half-links pattern to 3-D substrates for both silver and gold. We successfully etched the silver-coated glass capillaries using an aqueous ferricyanide etchant with high selectivity, as can be seen in Figure 19. Likewise, the cyanide etchant effectively etched the half-links design in gold on a glass capillary (see Figure 20). Two capillaries patterned with the half-links design can be aligned and adhered together, matching their patterns to form full links of an interlocking chain. Electroplating can be employed to build up the thickness of the half-links until they are connected. Dissolving the underlying glass capillary can produce a linear, interlinked chain.

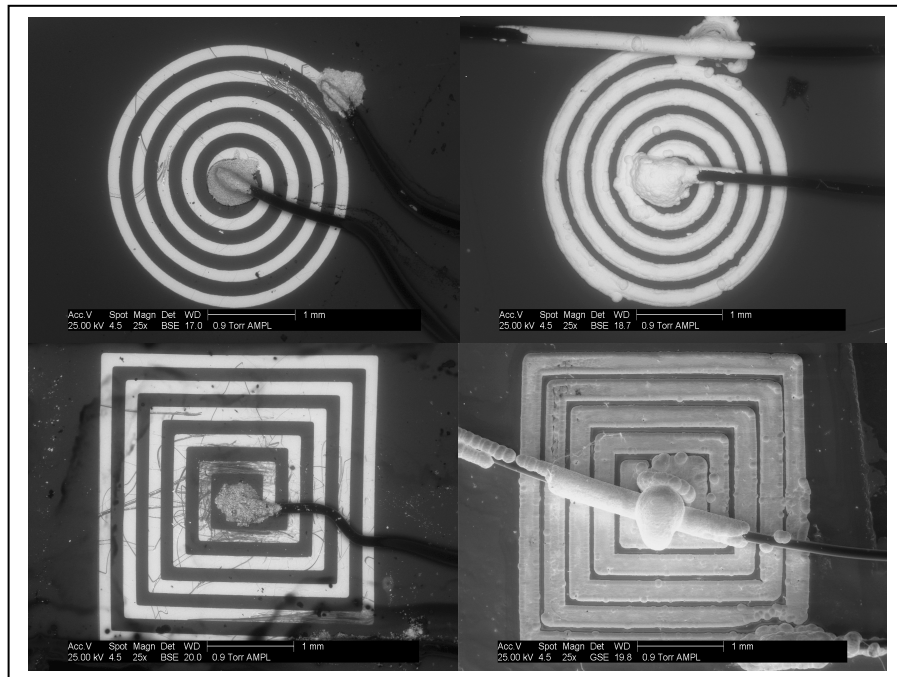


Figure 18. Round and square microcoils, after etching (left) and after electroplating (right). The wire width is $\sim 130 \mu\text{m}$ after etching and $\sim 220 \mu\text{m}$ after electroplating.

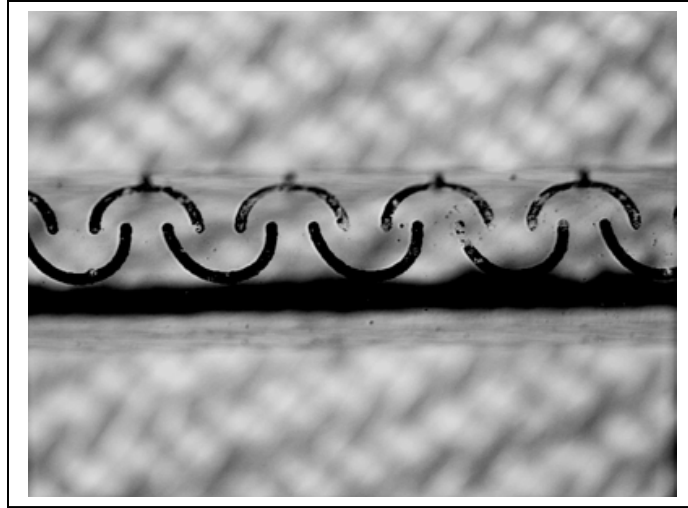


Figure 19. Optical micrograph of silver half-links design on a glass capillary.

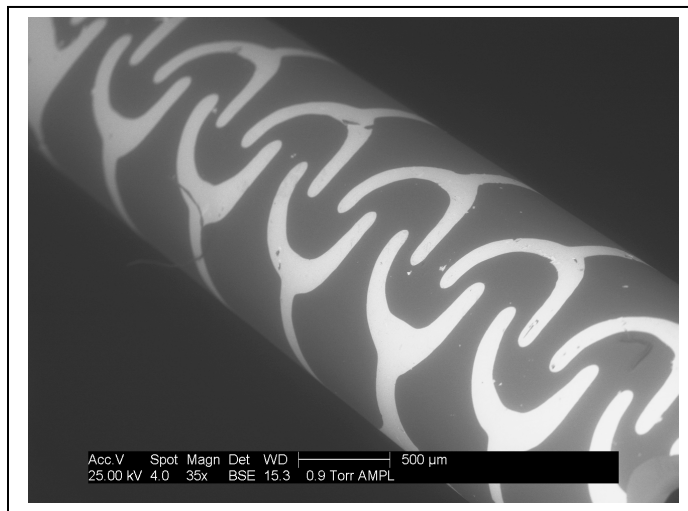


Figure 20. SEM image of gold half-links pattern on a glass capillary (with underlying Ti adhesion layer still present).

Jackman et al. [20] fabricated microchains by transferring a half-links design to each of two silver-coated glass capillaries and then joining them. In this design, they exploited the fact that two adjoining cylinders are topologically equivalent to two intersecting planes (see Figure 21). Instead of using microcontact printing to transfer the pattern to the

silver-coated capillaries, they coated each capillary uniformly with a photoresist and then carefully wrapped a patterned flexible photomask around the capillary. UV exposure through the clear areas of the photomask and subsequent development in a suitable solvent created the desired pattern in the photoresist. Two patterned capillaries were then aligned and adhered together, with their patterns matched to form the template for an interlinked chain. Electroplating nickel in areas defined by the patterned photoresist connected the two halves of each link and built up the thickness of the parts. Dissolution of the photoresist and glass capillaries resulted in a free-standing, interlinked microchain.

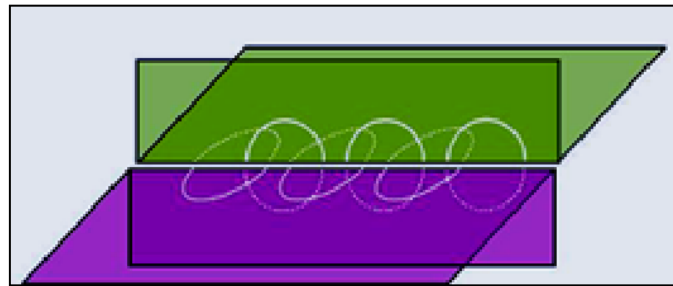


Figure 21. Drawing of the half-links pattern on two adjoining corners. The topology is the same for two adjoining cylinders.

This method is difficult and not easily repeatable. In addition, they had to attach a wire to each half-link by hand to get electrical continuity for the electroplating. We modified their method to make it more amenable to a manufacturing environment. We pursued the fabrication of microchains to investigate the feasibility of manufacturing a complex 3-D part. We designed a stamp that the capillary could roll over to transfer the half-links pattern. Our original design was intended to include a small wire coming from each half-link to provide electrical continuity for the electroplating process. As can be seen in Figure 16, we inadvertently omitted the wires for the outer set of half-links. We modified our design to include wires for all of the half-links, as well as contact cuffs at each end. Figure 22 shows the design of the elevated features of the stamp, which corresponds to the pattern created by the SAM.

We aligned and joined several pairs of patterned capillaries using silver epoxy. This maintained electrical continuity for the subsequent electroplating operations. Our parts produced electrically continuous structures. However, we were unable to build up the thickness of the gold enough to connect the half-links during electroplating. The geometry of the long, thin capillaries proved problematic for our traditional electroplating setup. Even after several hours in a gold cyanide bath, there was not an appreciable increase in the gold thickness. Troubleshooting efforts did not reveal the source of the problem.

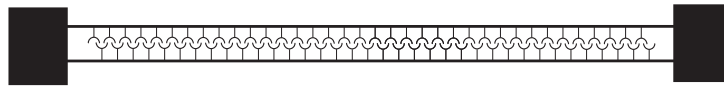


Figure 22. Modified design of the half-links pattern. This design includes wires and contact cuffs for the electroplating process.

We fabricated several 3-D microcoils using microcontact printing. We created a single helix by rolling a gold-coated capillary at a specified angle over the raised parallel lines of the stamp (see Figure 23). After numerous futile attempts to transfer the microcoil pattern by hand, a micromanipulator (see Figure 10) was employed to get proper alignment of the capillary on the stamp.

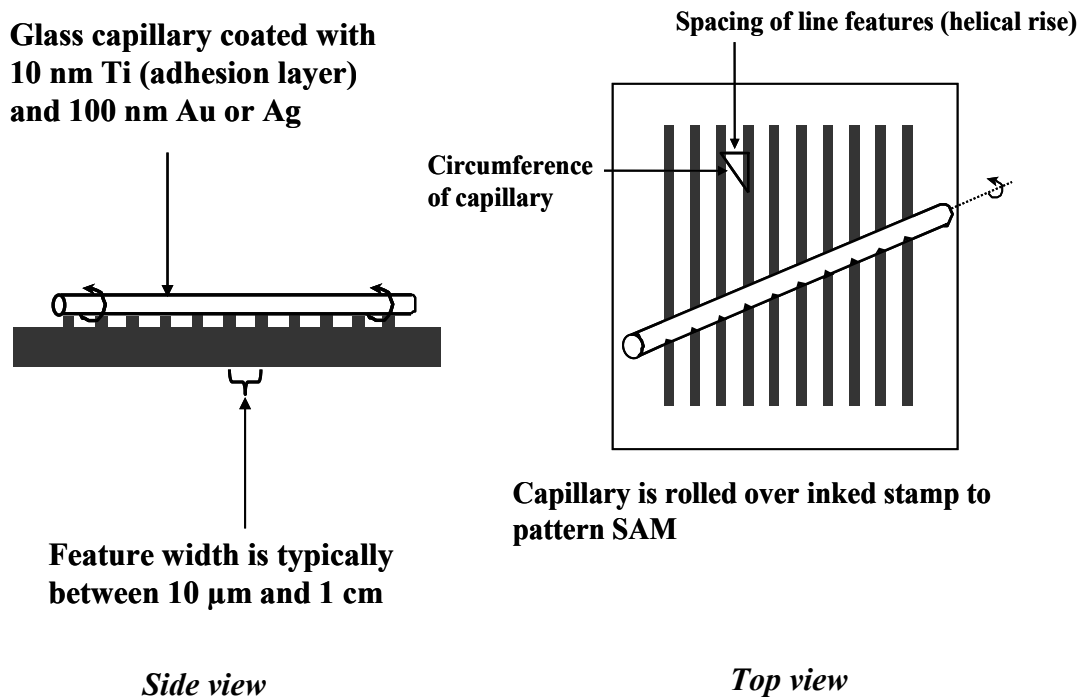


Figure 23. Microcontact-printing method for transferring the microcoil design to a metallized glass capillary.

The angle of rotation was calculated for each capillary using the following equation from Rogers et al. [25]:

$$\sin \theta = \frac{nd}{2\pi r}$$

where θ is the angle between the axis of the capillary and a horizontal line which intersects the vertical lines of the stamp (dotted line in Figure 24), $n=1$ for a single helix, d is the spacing between the lines (see Figure 24), and r is the radius of the capillary. For example, the desired angle of rotation is 3.42 degrees for a 1.6-mm-diameter capillary rolled over a stamp that has 300- μm -wide spaces between the lines.

Figure 25 shows the pattern for a helical coil in gold on a glass capillary; the bright lines are the gold and the thin dark lines are the underlying titanium. We used the contact-inking method to ink the stamp for this part. The capillary was rolled over the inked stamp using the micromanipulator. The computer-driven controller set the angle of rotation of the stamp with respect to the capillary. This type of helical structure can be used as a microcoil or a microspring, depending on the strength of the material deposited on the pattern during electroplating operations. Rogers et al. [22] fabricated silver microsprings which could be elastically stretched by more than 100%. They were able to build up the thickness of the silver by a few hundred microns by electroplating.

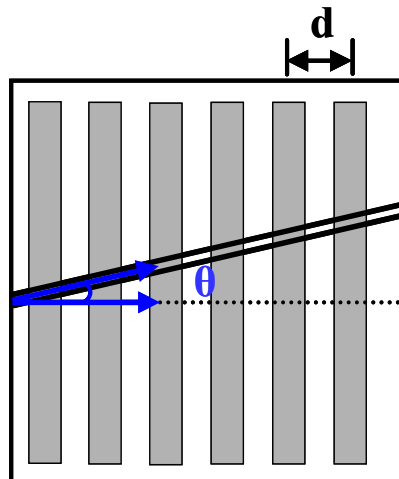


Figure 24. Diagram showing the parameters for rolling a capillary on a stamp to print the microcoil pattern.

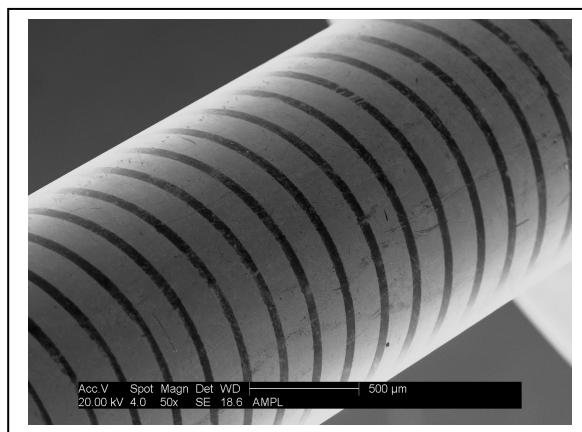


Figure 25. Etched microcoil pattern in gold on a capillary.

Several factors are critical in effectively transferring the microcoil pattern to a metallized capillary. If the capillary is not placed on the stamp at the desired angle, the printed pattern of parallel lines will not match up to form a helix (see lower left corner in Figure 26). The micromanipulator provided precise rotation of the rotary stage with respect to the capillary for transferring the microcoil pattern. However, there was no way to accurately align the stamp on the rotary stage in a reproducible manner.

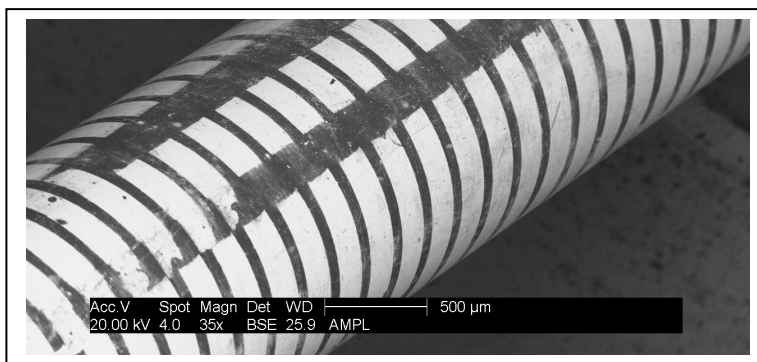


Figure 26. Examples of microcoil defects.

Another factor we found to be important in printing capillaries was the uniformity of thickness from one end of the stamp to the other end. If the stamp is too thick at one end, this causes the capillary to push down too hard on the stamp at that end (right-hand side of Figure 27), thereby distorting the pattern. In the worst case, this results in a solid gold band on that end of the capillary (with no pattern at all) after etching. At the thinner end of the stamp (left-hand side of Figure 27), the capillary skips over the stamp, causing

discontinuities in the pattern (shown as dark horizontal bands in upper quadrant of Figure 26). Once a stamp design is established for a particular application, a closed metal mold can be constructed to ensure dimensional stability and a uniform thickness of the stamp. The mold design must include a way to secure the master (a photoresist-covered silicon wafer) inside the mold without damaging it.

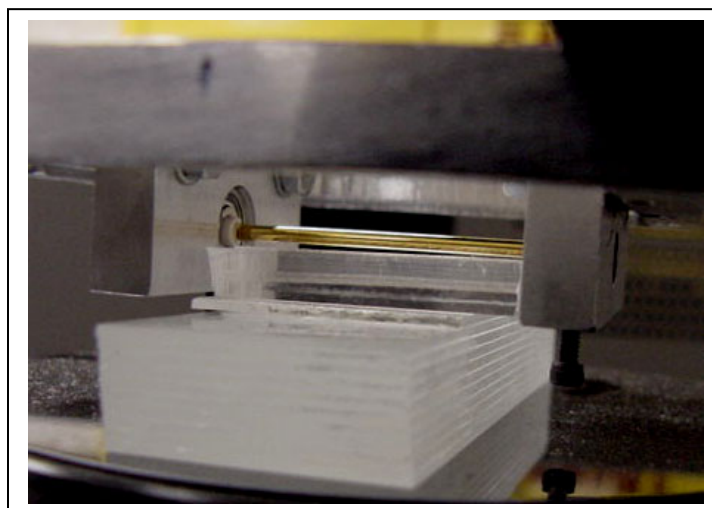


Figure 27. Uneven thickness of the stamp causes discontinuous contact of the capillary during printing.

We found that the contact-inking technique developed by Libioule et al. [11] markedly improved the resolution of fine features by minimizing the adversarial effects produced in the wet-inking process due to stray diffusion of HDT molecules. We used an inking time of 40 to 60 seconds and a contact time of 45 seconds. A longer contact time increased the incidence of blurred regions in the printed pattern; apparently, it gave the HDT molecules time to diffuse outside the printed area. Libioule et al. used an inking time of 40 seconds and a contact time of 30 seconds.

We printed the designs in Figure 28 using the contact inking method. We initially tried the wet-inking method to print these patterns with no success; there was no evidence of a printed pattern at all after etching. The stamp for these patterns was made from a master produced by photolithography using a chrome photomask. For some samples, a slight skipping of the stamp on the substrate produced a second pattern that was superimposed on the first (see Figure 29). The images in Figures 28 and 29 were obtained using backscattered-electron emission on the SEM, which detects differences in atomic number (Z) for the materials present in a particular sample. The bigger the nucleus, the more the electrons are elastically scattered. Therefore, a high- Z material such as gold ($Z=79$) produces a bright image against a low- Z background material such as titanium ($Z=22$).

Since the backscattered-electron imaging can detect differences in atomic number, we were able to determine that the material surrounding the stick figures is residual gold that remained on the surface after etching. Longer etching times may have removed this residual layer, at the risk of losing the pattern completely if the sample was left in the

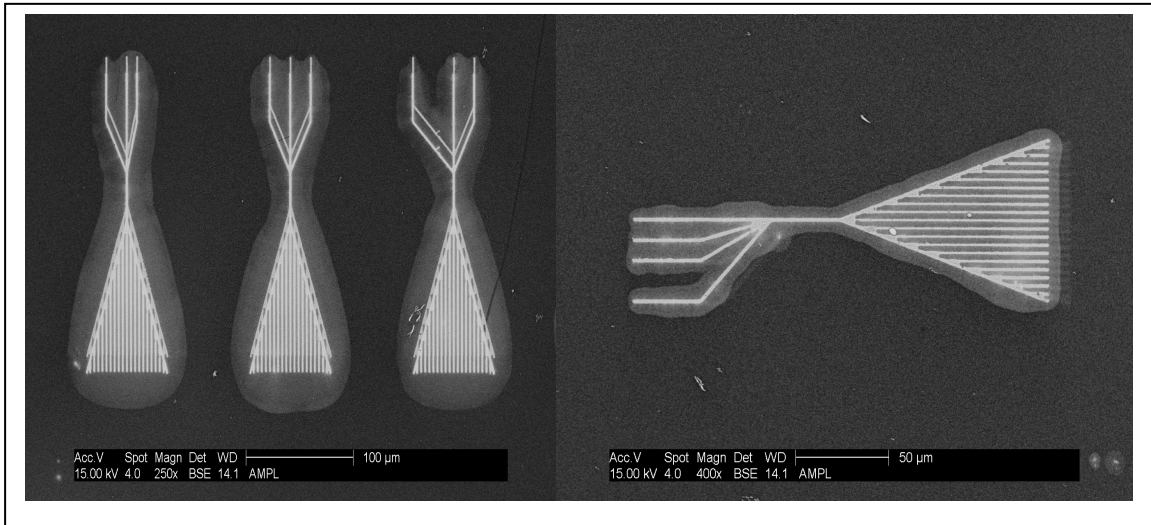


Figure 28. Etched patterns of stick figures printed on a gold substrate using the contact-inking method.

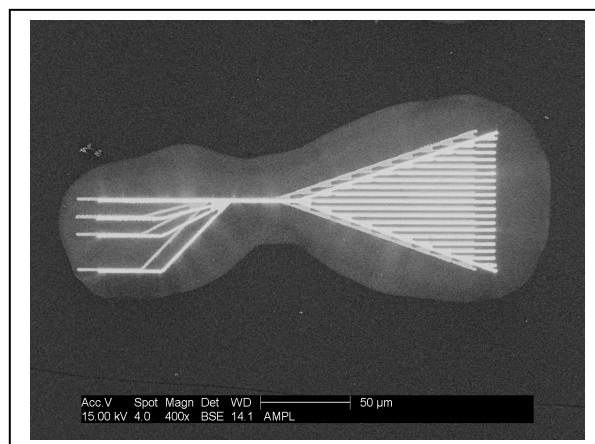


Figure 29. Example of a defect due to the stamp skipping on the substrate during printing.

etchant too long. The average width of six lines in the center of the “skirt” for a stick figure (see Figure 30) is 1.2 μm . This image was obtained using backscattered-electron emission on the SEM. As can be seen in these images, the Sylgard 184 did an excellent job of replicating the features of the master and subsequently transferring the pattern to a gold substrate for features as small as 1.2 μm .

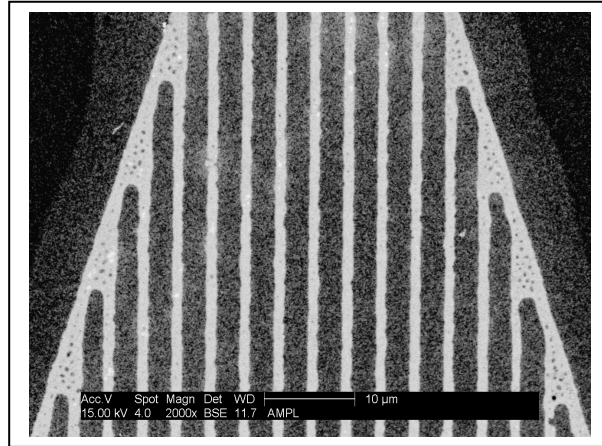


Figure 30. The average line width is 1.2 μm for the lines in the “skirt” area of the stick figures shown in Figures 28 and 29.

Conclusions and Recommendations for Future Work: Try Contact Inking with ECT and a Stiffer Stamp Material

The flexible photomasks that we used to make the masters worked well for rapid production of simple patterns with features in the range of tens of microns or more. The time and expense involved in generating a chrome mask was a significant barrier to using one during our development of different patterns. However, a chrome mask can be made once the details of a design have been finalized. This would provide better dimensional stability and greatly improve the quality of the master. A more precisely fabricated master would make a better stamp, which would result in a cleaner pattern transfer for fine features.

A more precise method of alignment of the stamp on the rotary stage of the micromanipulator would give better reproducibility of the pattern transfer when printing 3-D substrates. We recommend using a micromanipulator such as the one employed by Rogers et al. [24]. Their apparatus incorporates a laser to ensure proper alignment of the stamp and the capillary on the rotation and translation stages. They also have a CCD camera connected to a microscope and a video display to watch the printing process.

The Sylgard 184 worked very well as the stamp material for our applications; however, we believe 1- μm -wide features are close to the minimum size possible for this material to replicate. The formation of structures smaller than 1 μm requires the fabrication of stamps that are stiffer than Sylgard 184. Schmid et al. [13] found great success in printing features as small as 80 nm using a stiffer stamp. They developed a PDMS formulation using vinyl copolymers to make a new stamp material. The new formulation was made to provide greater stiffness without losing the ability to conform to a substrate. Incorporating glass nanoparticles into their formulation resulted in a material with a compression modulus of 9.7 N/mm². This is much greater than that for Sylgard 184 (2 N/mm²), which is formulated from a vinyl-terminated prepolymer and filled with silica nanoparticles.

We recommend trying ECT as the alkanethiol for printing features less than 1 μm , either instead of HDT, or mixed with HDT. The vapor pressure of ECT ($\sim 1 \times 10^{-9}$ kPa at 25°C according to Delamarche et al. [4]) is about 10³ kPa lower than that of HDT ($\sim 1.4 \times 10^{-6}$ kPa at 25°C [48]). Therefore, it is not as volatile as HDT, and not as diffusive. As expected, there is a decrease in vapor pressure with an increase in molecular weight (314.62 for ECT compared with 258.51 for HDT). Libioule et al. [11] printed 100-nm-wide gold lines by using the contact-inking technique with a 1:1 solution of HDT:ECT in ethanol. They found that this mixed SAM maintained good protection of gold during wet etching. They used a PDMS copolymer formulation such as the one developed by Schmid et al. [13] to make a stiffer stamp for this application. Li et al. [28] successfully printed ECT on a gold surface to create features as small as 100 nm. They also used a PDMS copolymer formulation such as the one developed by Schmid et al. [13] to make a stiffer stamp for their work.

One disadvantage of ECT is that it is a solid at room temperature, so it requires some agitation in a solvent to prepare the ink solution. Delamarche et al. [4] sonicated solutions of ECT in ethanol for 5 minutes to help dissolve the ECT. Using a 0.2 mM solution of ECT in ethanol and a contact time of 3 seconds, they were able to print an array of 0.6 $\mu\text{m} \times 3 \mu\text{m}$ dots using a Sylgard 184 stamp. They measured an increase in dimensions of the printed shape of $0.1 \pm 0.05 \mu\text{m}$ in all directions. In further efforts, they were able to make a stamp with features as small as 50 nm using a PDMS copolymer formulation such as the one developed by Schmid et al. [13]. The printed ECT patterns resulted in broadening of features. For example, 50-nm-diameter dots on the stamp produced dots of diameters $90 \pm 10 \text{ nm}$ in the etched gold. Furthermore, many of the gold dots had irregular shapes. This shows the lower limit of feature size possible with microcontact printing of alkanethiolates on gold, even with a stiffer stamp.

We suggest exploring the use of other metals besides gold to find a more robust thin-film material that can be patterned by microcontact printing, and can withstand the process of bonding wires to the final part. For example, Goetting et al. used microcontact printing to transfer SAMs of alkanephosphonic acids to aluminum [49] and also alkanethiolates to palladium according to Xia et al. [1]. Even though we successfully patterned both silver and gold, we used gold primarily because the turnaround for the thin-film deposition was much quicker for gold than for silver. Copper produced poor pattern transfer due to poor

selectivity in the wet etching. Xia et al. [42] also found copper problematic. They used a 2 mM solution of HDT in ethanol to create a variety of test patterns in gold, silver, and copper; the selectivity and edge resolution were excellent for both silver and gold, but were much poorer for copper. Rogers et al. [23] fabricated microcoils of 70- μm -wide printed wires on glass capillaries. After electroplating the silver microcoil pattern with a thin ($\sim 1 \mu\text{m}$) layer of gold and then a thick ($\sim 10 \mu\text{m}$) layer of copper, the wire was strong enough to be peeled back from the ends and used to connect the microcoil to a data-acquisition circuit. This shows a creative way to produce a copper microcoil without having to produce a copper pattern with microcontact printing and selective etching. Laibinis et al. [50, 51] compared the structures and wetting properties of alkanethiolate SAMs on copper, silver, and gold. We discovered a valuable observation by Ostuni et al. [31] for those interested in biological applications of microcontact printing. They found that gold substrates covered with alkanethiolate SAMs are not toxic to living cells; however, silver substrates covered with alkanethiolate SAMs release an ion that is toxic to cells when the substrates are placed in biological solutions.

Attempts to electroplate a uniform thickness of gold on capillaries were not successful using our traditional setup. We suggest using computer-controlled electroplating equipment such as a Voltalab system (Radiometer Analytical, Villeurbanne, France), which provides a real-time display of the operating parameters. We recommend using a setup with a rotating electrode for plating long, thin cylindrical parts; this would improve the uniformity of the coating by spinning the part while plating it. The rate of rotation could be optimized for a particular application. A special fixture would be required to allow the rotating electrode to hold a capillary.

Ultra-precision micromachining is a promising microfabrication technique for making microcoils with fine wires because of its accuracy and speed. FIB sputtering can create tool shapes that are not easily fabricated by conventional methods such as polishing and grinding. In the FIB sputtering process, a 20-keV gallium beam is directed at the part in several steps to create a number of critically-aligned facets. Material can either be added or removed in this technique. Numerically-controlled, ultra-precision machining with a microgrooving tool produces a close correspondence between the tool width and the resulting feature size. Adams et al. [52] formed helical grooves on a PMMA cylinder using a tungsten carbide microgrooving tool made by FIB sputtering. The grooves were 13.1 μm wide and 4 μm deep. They were able to produce a near-rectangular cross section in the grooves. SEM measurements showed that the micromachined groove width of 13.1 μm was close to the tool width of 13.0 μm . In further work, Picard et al. [53] created a microcoil by removing a conductive layer in a helical pattern on a 3-mm-diameter copper-coated PMMA cylinder. They used FIB sputtering to remove the copper down to the PMMA surface. The wire width was determined by the pitch of the turning operation. The rectangular cross-section of the wire was 45 μm by 15 μm and the pitch was 74 μm . The solid areas of copper remaining at the ends of the helical structure could act as contact cuffs for wire bonding. FIB sputtering and ultra-precision micromachining can produce microcoils with high precision and excellent reproducibility.

Potential applications for microcoils at Sandia include microtransformers for flyback voltage-conversion circuits, which could be used in miniature capacitive-discharge units [54]. The advantage of 3-D microcoils made on glass capillaries is the capability to fill the hollow center with a magnetic core material for transformer applications. The advantage of flat microcoils is that they are compact; many microcoils can be stacked on top of each other or other microcomponents in a tight space. For both 2-D and 3-D microcoils, a robust method must be developed to attach wires securely to the ends of the microcoils before their use in microcomponents is feasible. Lochel et al. [55] used surface micromachining to construct a flat microcoil with an integrated contact bridge that connected the inner wire of the coil to an outer contact or bond pad. Their process included photolithographic patterning of a thick layer of photoresist followed by electroplating on the patterned surface. Electrodeposited sacrificial layers were used to create a free-standing 1.8-mm-long contact bridge that stood 55 μm above the surface of the microcoil. If a similar idea of a contact bridge could be incorporated in the design of a flat microcoil, then wires could easily be bonded to bond pads without damaging the microcoil. If a method for securely attaching wires to microcoils is developed, this will greatly increase the likelihood that microcoils will be used in a microcomponent application.

A helical microspring could be used in environmental sensing devices at Sandia as a replacement of the folded-beam type spring. One advantage of the helical spring is that it exerts a force along one axis only. In addition, it has a longer linear range than the folded-beam type springs. In order to utilize microsprings, a closed loop on each end of the spring needs to be included in the design so that it can be gripped by the assembler and installed in the desired position.

It should be noted that we do not propose microcontact printing as a replacement for LIGA, which still reigns as the method for generating high-aspect-ratio features; it is rather a complementary microfabrication technique. Microcontact printing looks promising for constructing single-level structures such as microelectrode arrays and sensors. It can be a viable technique for creating 3-D structures such as microcoils and microsprings if the right equipment is available to achieve proper alignment of the stamp and capillary during printing, and if a means is available to connect them to other parts in subsequent assembly operations. Microcontact printing provides a wide variety of new opportunities in the fabrication of microcomponents, and increases the options of designers.

References

1. Xia, Y. and G.M. Whitesides, *Soft Lithography*. Angewandte Chemie International Edition, 1998. **37**: p. 550-575.
2. Biebuyck, H.A., et al., *Lithography beyond light: Microcontact printing with monolayer resists*. IBM Journal of Research & Development, 1997. **41**(1/2): p. 159-170.
3. Brittain, S.T., et al., *Microorigami: Fabrication of Small, Three-Dimensional, Metallic Structures*. Journal of Physical Chemistry B, 2001. **105**(2): p. 347-350.
4. Delamarche, E., et al., *Transport Mechanisms of Alkanethiols during Microcontact Printing on Gold*. Journal of Physical Chemistry B, 1998. **102**(18): p. 3324-3334.
5. Gorman, C.B., H.A. Biebuyck, and G.M. Whitesides, *Use of a Patterned Self-Assembled Monolayer To Control the Formation of a Liquid Resist Pattern on a Gold Surface*. Chemistry of Materials, 1995. **7**(2): p. 252-254.
6. Huck, W.T.S., et al., *Patterned Polymer Multilayers as Etch Resists*. Langmuir, 1999. **15**(20): p. 6862-6867.
7. Jackman, R.J., J.L. Wilbur, and G.M. Whitesides, *Fabrication of Submicrometer Features on Curved Substrates by Microcontact Printing*. Science (Washington, D. C., 1883-), 1995. **269**: p. 664-666.
8. Jackman, R.J., S.T. Brittain, and G.M. Whitesides, *Fabrication of Three-Dimensional Microstructures by Electrochemically Welding Structures Formed by Microcontact Printing on Planar and Curved Substrates*. Journal of Microelectromechanical Systems, 1998. **7**(2): p. 261-266.
9. Kumar, A. and G.M. Whitesides, *Features of gold having micrometer to centimeter dimensions can be formed through a combination of stamping with an elastomeric stamp and an alkanethiol "ink" followed by chemical etching*. Applied Physics Letters, 1993. **63**(14): p. 2002-2004.
10. Kumar, A., H.A. Biebuyck, and G.M. Whitesides, *Patterning Self-Assembled Monolayers: Applications in Materials Science*. Langmuir, 1994. **10**(5): p. 1498-1511.
11. Libioulle, L., et al., *Contact-Inking Stamps for Microcontact Printing of Alkanethiols on Gold*. Langmuir, 1999. **15**(2): p. 300-304.
12. Moffat, T.P. and H. Yang, *Patterned Metal Electrodeposition Using an Alkanethiolate Mask*. Journal of Electrochemical Society, 1995. **142**(11): p. L220-L222.
13. Schmid, H. and B. Michel, *Siloxane Polymers for High-Resolution, High-Accuracy Soft Lithography*. Macromolecules, 2000. **33**(8): p. 3042-3049.
14. Wilbur, J.L., et al., *Microfabrication by Microcontact Printing of Self-Assembled Monolayers*. Advanced Materials (Weinheim, Federal Republic of Germany), 1994. **6**(7/8): p. 600-604.
15. Wilbur, J.L., et al., *Microcontact printing of self-assembled monolayers: applications in microfabrication*. Nanotechnology, 1996. **7**: p. 452-457.
16. Xia, Y., et al., *Microcontact Printing of Alkanethiols on Copper and Its Application in Microfabrication*. Chemistry of Materials, 1996. **8**(3): p. 601-603.

17. Xia, Y., X.-M. Zhao, and G.M. Whitesides, *Pattern transfer: Self-assembled monolayers as ultrathin resists*. *Microelectronic Engineering*, 1996. **32**: p. 255-268.
18. Breen, T.L., et al., *Design and Self-Assembly of Open, Regular, 3D Mesostructures*. *Science (Washington, D. C., 1883-)*, 1999. **284**: p. 948-951.
19. Jackman, R.J., J.A. Rogers, and G.M. Whitesides, *Fabrication and Characterization of a Concentric Cylindrical Microtransformer*. *IEEE Transactions on Magnetics*, 1997. **33**(4): p. 2501-2503.
20. Jackman, R.J., et al., *Design and Fabrication of Topologically Complex, Three-Dimensional Microstructures*. *Science (Washington, D. C., 1883-)*, 1998. **280**: p. 2089-2091.
21. Johansen, L.S., et al., *Electroforming of 3D microstructures on highly structured surfaces*. *Sensors and Actuators, A: Physical*, 2000. **83**: p. 156-160.
22. Rogers, J.A., R.J. Jackman, and G.M. Whitesides, *Microcontact Printing and Electroplating on Curved Substrates: Production of Free-Standing Three-Dimensional Metallic Microstructures*. *Advanced Materials (Weinheim, Federal Republic of Germany)*, 1997. **9**(6): p. 475-477.
23. Rogers, J.A., et al., *Using microcontact printing to fabricate microcoils on capillaries for high resolution proton nuclear magnetic resonance on nanoliter volumes*. *Applied Physics Letters*, 1997. **70**(18): p. 2464-2466.
24. Rogers, J.A., et al., *Using microcontact printing to generate amplitude photomasks on the surfaces of optical fibers: A method for producing in-fiber gratings*. *Applied Physics Letters*, 1997. **70**(1): p. 7-9.
25. Rogers, J.A., R.J. Jackman, and G.M. Whitesides, *Constructing Single- and Multiple-Helical Microcoils and Characterizing Their Performance as Components of Microinductors and Microelectromagnets*. *Journal of Microelectromechanical Systems*, 1997. **6**(3): p. 184-192.
26. Wu, H., et al., *Fabrication of Topologically Complex Three-Dimensional Microstructures: Metallic Microknots*. *Journal of the American Chemical Society*, 2000. **122**(51): p. 12691-12699.
27. Wu, H., S.H. Whitesides, and G.M. Whitesides, *Fabrication of Micro-Chain Mail by Simultaneous, Patterned Electrodeposition on a Plane and Multiple Cylinders*. *Angew. Chem. Int. Ed.*, 2001. **40**(11): p. 2059-2060.
28. Li, S.P., et al., *Magnetic nanostructure fabrication by soft lithography and vortex-single domain transition in Co dots*. *Journal of Magnetism and Magnetic Materials*, 2002. **241**: p. 447-452.
29. Kumar, A., et al., *Patterned Self-Assembled Monolayers and Meso-Scale Phenomena*. *Accounts of Chemical Research*, 1995. **28**(5): p. 219-226.
30. Lahiri, J., E. Ostuni, and G.M. Whitesides, *Patterning Ligands on Reactive SAMs by Microcontact Printing*. *Langmuir*, 1999. **15**(6): p. 2055-2060.
31. Ostuni, E., L. Yan, and G.M. Whitesides, *The interaction of proteins and cells with self-assembled monolayers of alkanethiolates on gold and silver*. *Colloids and Surfaces B: Biointerfaces*, 1999. **15**(1): p. 3-30.
32. Yan, L., et al., *Patterning Thin Films of Poly(ethylene imine) on a Reactive SAM Using Microcontact Printing*. *Langmuir*, 1999. **15**(4): p. 1208-1214.

33. Hovis, J.S. and S.G. Boxer, *Patterning Barriers to Lateral Diffusion in Supported Lipid Bilayer Membranes by Blotting and Stamping*. Langmuir, 2000. **16**(3): p. 894-897.
34. Deng, T., et al., *Using Patterns in Microfiche as Photomasks in 10-micron-Scale Microfabrication*. Langmuir, 1999. **15**(19): p. 6575-6581.
35. Delamarche, E., et al., *Stability of Molded Polydimethylsiloxane Microstructures*. Advanced Materials (Weinheim, Federal Republic of Germany), 1997. **9**(9): p. 741-746.
36. Ulman, A., *An Introduction to Ultrathin Organic Films From Langmuir-Blodgett to Self-Assembly*. 1991, Academic Press, Inc.: San Diego, CA. p. 237.
37. Kumar, A., et al., *The Use of Self-Assembled Monolayers and a Selective Etch To Generate Patterned Gold Features*. Journal of the American Chemical Society, 1992. **114**: p. 9188-9189.
38. Ulman, A., *An Introduction to Ultrathin Organic Films From Langmuir-Blodgett to Self-Assembly*. 1991, Academic Press, Inc.: San Diego, CA. p. 280.
39. Ulman, A., *An Introduction to Ultrathin Organic Films From Langmuir-Blodgett to Self-Assembly*. 1991, Academic Press, Inc.: San Diego, CA. p. 293.
40. Larsen, N.B., et al., *Order in Microcontact Printed Self-Assembled Monolayers*. Journal of the American Chemical Society, 1997. **119**(13): p. 3017-3026.
41. Eberhardt, A.S., et al., *Defects in Microcontact-Printed and Solution-Grown Self-Assembled Monolayers*. Langmuir, 1999. **15**(5): p. 1595-1598.
42. Xia, Y., et al., *A Selective Etching Solution for Use with Patterned Self-Assembled Monolayers of Alkanethiolates on Gold*. Chemistry of Materials, 1995. **7**(12): p. 2332-2337.
43. Baca, J.T., *SAND2000-2029C: Microfabrication and Micropatterning with Soft Lithography*. 2000, Sandia National Laboratories: Albuquerque, NM.
44. Xia, Y., et al., *Use of Electroless Silver as the Substrate in Microcontact Printing of Alkanethiols and Its Application in Microfabrication*. Langmuir, 1998. **14**(2): p. 363-371.
45. Huang, J. and J.C. Hemminger, *Photooxidation of Thiols in Self-Assembled Monolayers on Gold*. Journal of the American Chemical Society, 1993. **115**(8): p. 3342-3343.
46. Shaw, M., et al., *Improving the Process Capability of SU-8*. 2001, MicroChem Corporation: Newton, MA.
47. *NANO SU-8 2000 Negative Tone Photoresists Formulations 2-15*. 2001, MicroChem Corporation: Newton, MA.
48. *Properties listed by CAS number*, in *Handbook of Physical Properties of Organic Chemicals*, P.H. Howard and W.M. Meylan, Editors. 1997, CRC Press, Inc.: Boca Raton, FL. p. 700.
49. Goetting, L.B., T. Deng, and G.M. Whitesides, *Microcontact Printing of Alkanephosphonic Acids on Aluminum: Pattern Transfer by Wet Chemical Etching*. Langmuir, 1999. **15**(4): p. 1182-1191.
50. Laibinis, P.E., et al., *Comparison of the Structures and Wetting Properties of Self-Assembled Monolayers of n-Alkanethiols on the Coinage Metal Surfaces, Cu, Ag, Au*. Journal of the American Chemical Society, 1991. **113**(19): p. 7152-7167.

51. Laibinis, P.E. and G.M. Whitesides, *ω -Terminated Alkanethiolate Monolayers on Surfaces of Copper, Silver, and Gold Have Similar Wettabilities*. Journal of the American Chemical Society, 1992. **114**(6): p. 1990-1995.
52. Adams, D.P., M.J. Vasile, and A.S.M. Krishnan, *Microgrooving and microthreading tools for fabricating curvilinear features*. Precision Engineering, 2000. **24**: p. 347-356.
53. Picard, Y.N., et al., *SAND2002-1258J: Focused Ion Beam Shaped Microtools for Ultra-Precision Machining of Cylindrical Components*. 2002, Sandia National Laboratories: Albuquerque, NM.
54. Oliver, A.D., *SAND2002-1398: Microtransformers: Technologies and Tradeoffs*. 2002, Sandia National Laboratories: Albuquerque, NM.
55. Lochel, B., et al., *Microcoils fabricated by UV depth lithography and galvanoplatin*. Sensors and Actuators, A: Physical, 1996. **54**: p. 663-668.

Distribution:

1 MS0328 W. C. Curtis III, 2612
1 0328 S. N. Pecak, 2612
1 0329 G. E. Sleafy, 2614
1 0428 E. H. Detlefs, 12301
1 0492 B. M. Mickelsen, 12332
1 0492 R. L. Myers, 12332
1 0492 F. M. Rosen, 12332
1 0516 M. B. Ritchey, 2564
1 0516 R. G. Spulak, 2564
1 0603 C. M. Matzke, 1763
1 0958 J. A. Emerson, 14172
1 0958 R. K. Giunta, 14172
1 0958 C. J. Rondeau, 14172
1 0958 J. A. Ruffner, 14172
1 0959 D. P. Adams, 14171
1 0959 A. L. Casias, 14171
1 0959 T. C. Gourley, 14171
1 0959 R. L. Poole, 14171
1 0959 B. L. Silva, 14171
1 0959 D. J. Staley, 14171
1 0959 R. N. Stokes, 14171
1 0959 M. J. Vasile, 14171
1 0961 C. L. J. Adkins, 14100
1 1076 T. A. Fischer, 1745
1 1076 A. D. Oliver, 1745
1 9403 L. A. Domeier, 8722

1 9018 Central Technical Files, 8945-1
2 0899 Technical Library, 9616
1 0612 Review & Approval Desk, 9612
For DOE/OSTI
1 0188 LDRD Office, 1011